Measurement of the W boson mass with the ATLAS detector

Francesco Giuli

Special INFN seminar
'Sapienza' University of Rome
10/05/2022

Motivation

- In the EW sector of the SM, the W mass at loop level is

$$m_W^2 = \frac{\pi\alpha}{\sqrt{2}G_F\left(1 - m_W^2/m_Z^2\right)\left(1-\Delta r\right)}$$

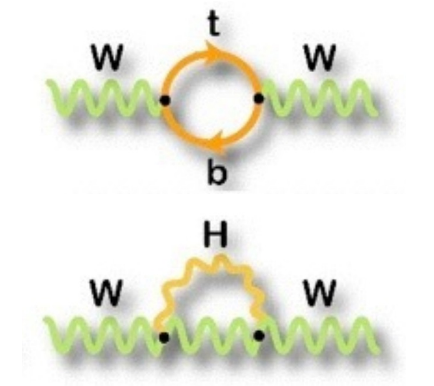

- Δr reflects loop corrections, depends on m_t^2 and $\ln(m_H)$

- The **relation between m_W, m_t, and m_H** provides **stringent test of the SM** and is **sensitive to New Physics**

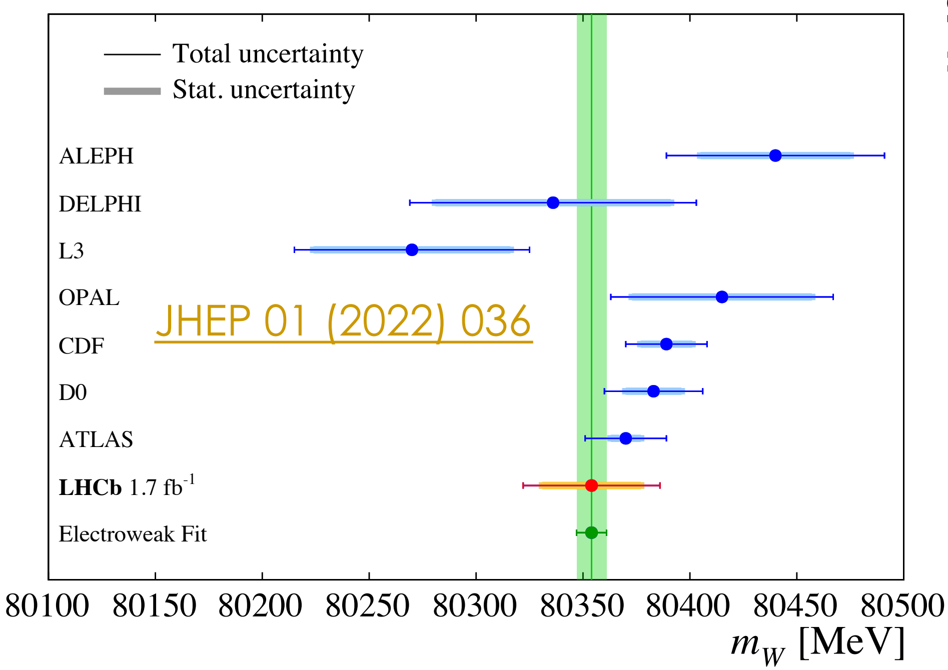

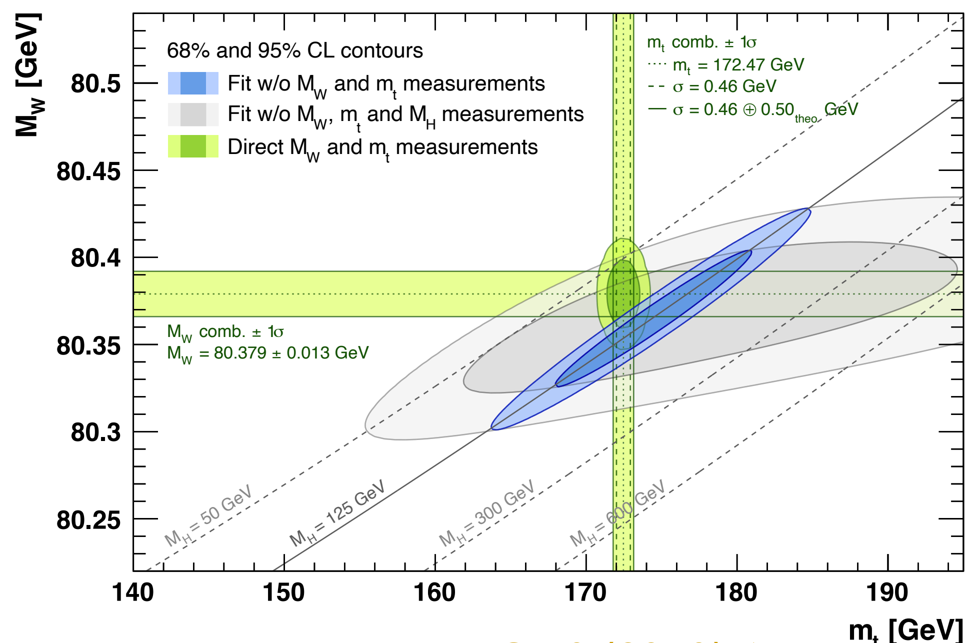

EPJC 78 (2018) 675

W mass at the LHC

- A pp **collider** is the **most challenging environment to measure** m_W, worse compared to e^+e^- and $p\bar{p}$

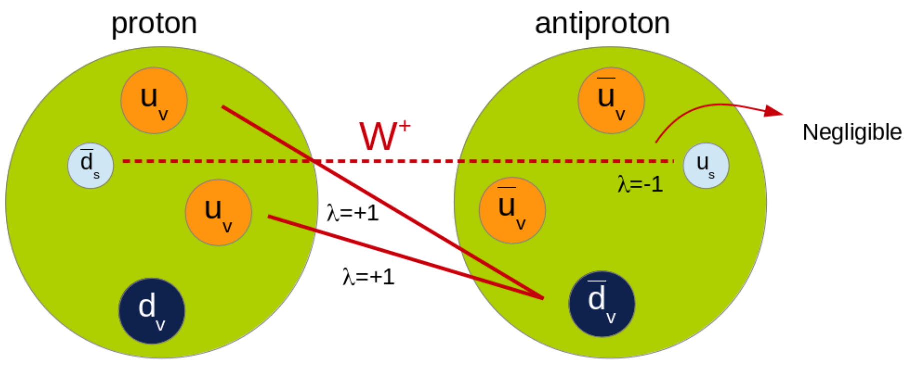

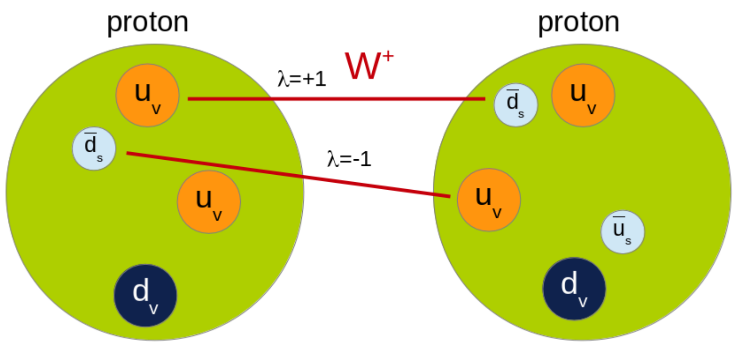

In $p\bar{p}$ collisions W bosons are mostly produced in the same helicity state

In pp collisions they are equally distributed between positive and negative helicity stes

Large PDF-induced W-polarisation uncertainty affecting the p_T lepton

Further QCD complications:

- **Heavy-flavour-initiated processes**
- W^+, W^- and Z produced by different light flavour fractions
- **Larger gluon-induced W production**

- First measurement of the W-boson mass in pp collisions at the LHC by ATLAS - EPJC 78 (2018) 110

Measurement overview

- Not possible to fully reconstruct m_W
- Sensitive final state distributions: $\boldsymbol{p_T^l, m_T}$ and $\boldsymbol{p_T^{miss}}$
- $\vec{p}_T^{miss} = -(\vec{p}_T^l + \vec{u}_T),\ m_T = \sqrt{2p_T^l p_T^{miss}(1-\cos\Delta\phi)}$
  being $\vec{u}_T$ the recoil
- Benefit from the fully reconstructed mass in Z boson sample to validate the analysis and provide significant experimental and theoretical constraints

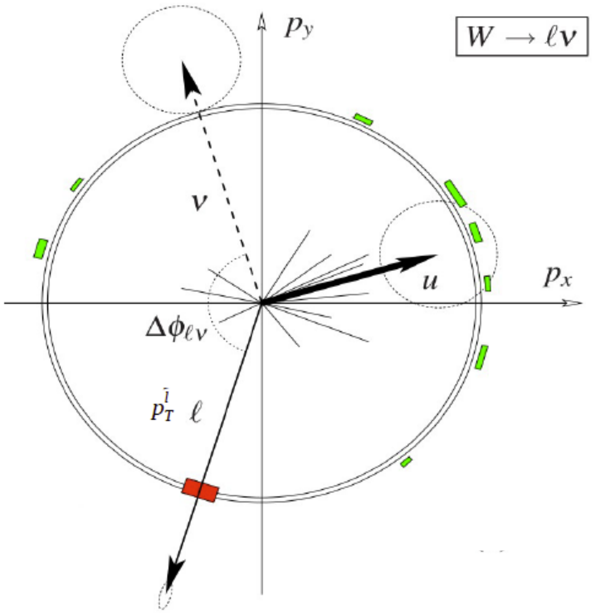

- Use **Z → ll events to calibrate the detector response to energy scales and resolutions** of the leptons and of the recoil
- Build the **physics modelling** by supplementing the MC samples with **higher order corrections and fits to DY ancillary measurements**
- Validate the physics modelling and calibration by extraction m_Z from p_T^l and m_T in the Z sample
- **Extract m_W in several categories and combine**

Physics modelling

- We call '**physics modelling**' the **theoretical prediction used to extract the W mass** from data, and the way theory uncertainties are addressed

- The DY cross section can be reorganised by factorising the dynamic of the boson production and the kinematic of the boson decay:

$$\frac{d\sigma}{dp_1\,dp_2} = \left[\frac{d\sigma(m)}{dm}\right]\left[\frac{d\sigma(y)}{dy}\right]\left[\frac{d\sigma(p_T, y)}{dp_T\,dy}\left(\frac{d\sigma(y)}{dy}\right)^{-1}\right]\left[(1+\cos^2\theta) + \sum_{i=0}^{7} A_i(p_T, y)P_i(\cos\theta, \phi)\right]$$

Breit-Wigner

NNLO pQCD

Parton Shower

NNLO pQCD

- This factorisation allows building a composite model, and using the most accurate model for each term

- **Fundamental** aspect of the model: the use of **ancillary DY measurement** for validation, fitting the free parameters of the model and assessing the uncertainties

- Within the W mass analysis, further validation of the model is provided by Z mass fits, W boson control plots and compatibility of m_W categories

Rapidity and angular coefficients

- The rapidity distribution and A_i coefficients modelled with **NNLO predictions** and the CT10nnlo PDF set

- PDF choice validated on the observed suppression of the strange quark in the W,Z cross-section data published by ATLAS - EPJC 77 (2017) 367

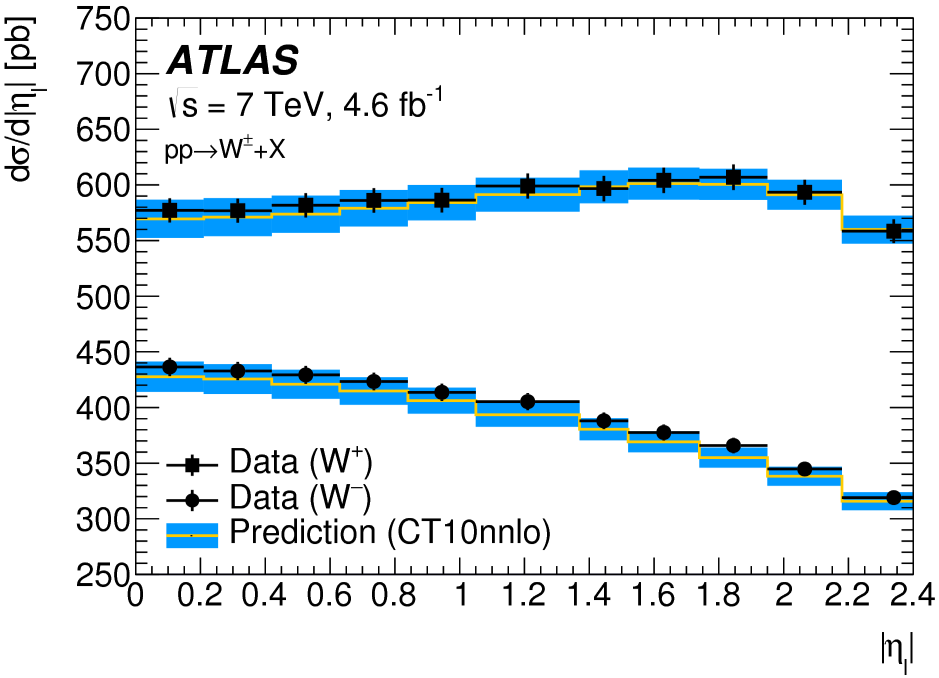

Satisfactory agreement between the theoretical predictions and the measurements: χ^2**/dof = 45/34**

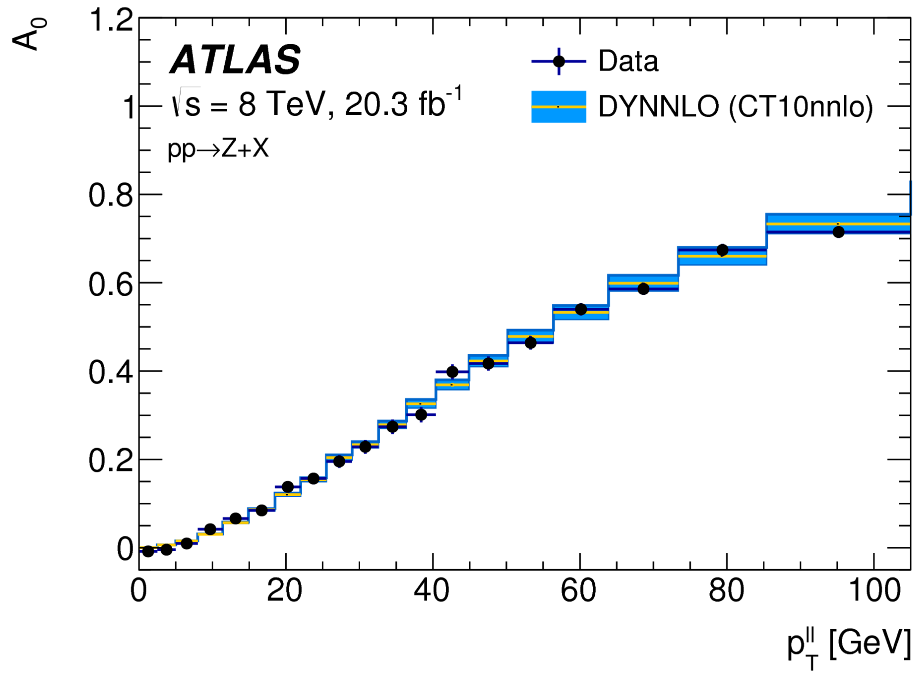

DYNNLO predictions validated by comparison to the A_i measurement at 8 TeV – JHEP 08 (2016) 159

Z transverse momentum

- The **Pythia8 parton shower** (PS) is used as model for the p_T^W
- The parameters of the model are fit to the 7 TeV p_T^Z measurement - AZ tune

JHEP 09 (2014) 145

	Pythia8
Tune Name	AZ
Primordial k_T [GeV]	1.71 ± 0.03
ISR $\alpha_S^{ISR}(m_Z)$	0.1237 ± 0.0002
ISR cut-off [GeV]	0.59 ± 0.08
$\chi^2_{min}/\mathrm{dof}$	45.4/32

- The **agreement** between data and Pythia8 AZ is **better than 1%** for p_T < 40 GeV
- Pythia8 is used to transfer from the p_T^Z to the p_T^W distribution and to evaluate theory uncertainties on the W/Z p_T ratio

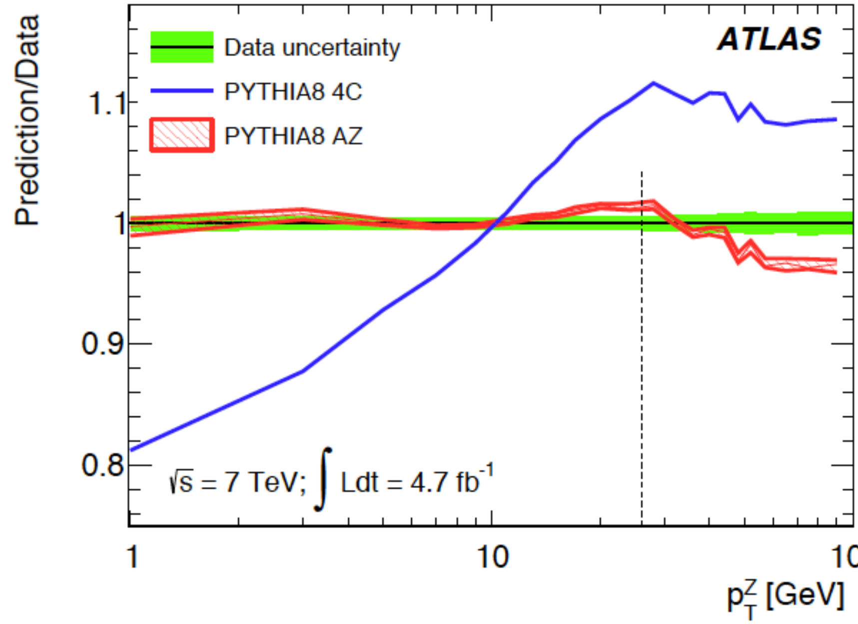

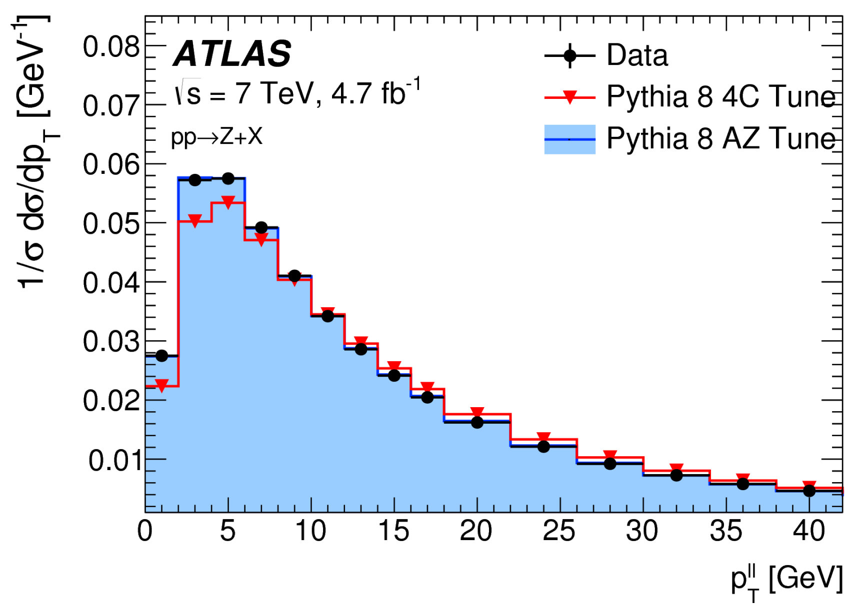

W transverse momentum

- The Pythia8 AZ tune is fixed by the p_T^Z data – extrapolate to W considering relative variations of the W and Z p_T distributions

- Resummed predictions (DYRES, ResBos, CuTe) and Powheg MiNLO + Pythia8 were tried but they predict harder p_T^W spectrum for a given p_T^Z spectrum

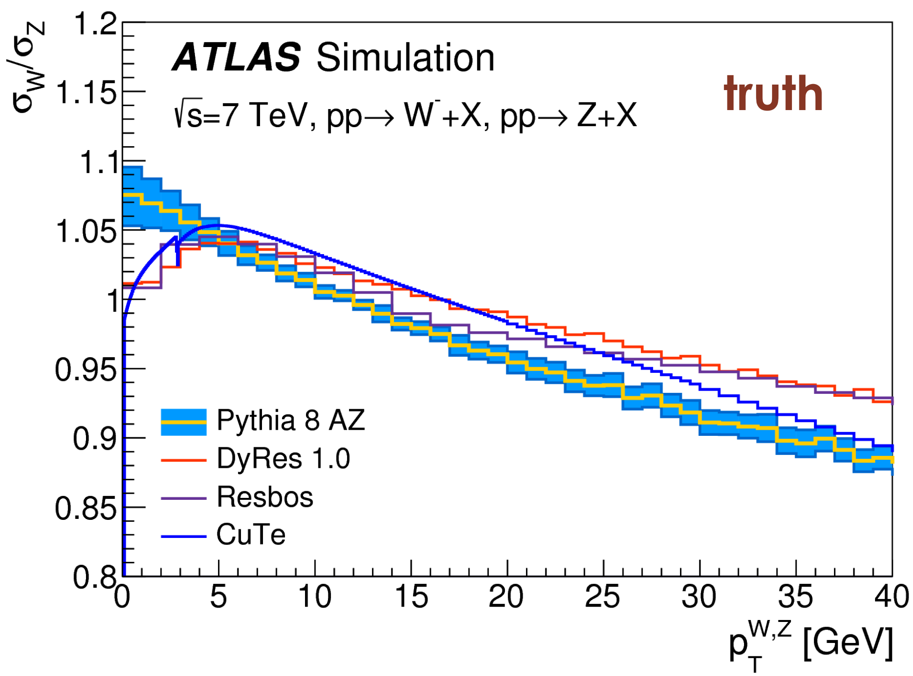

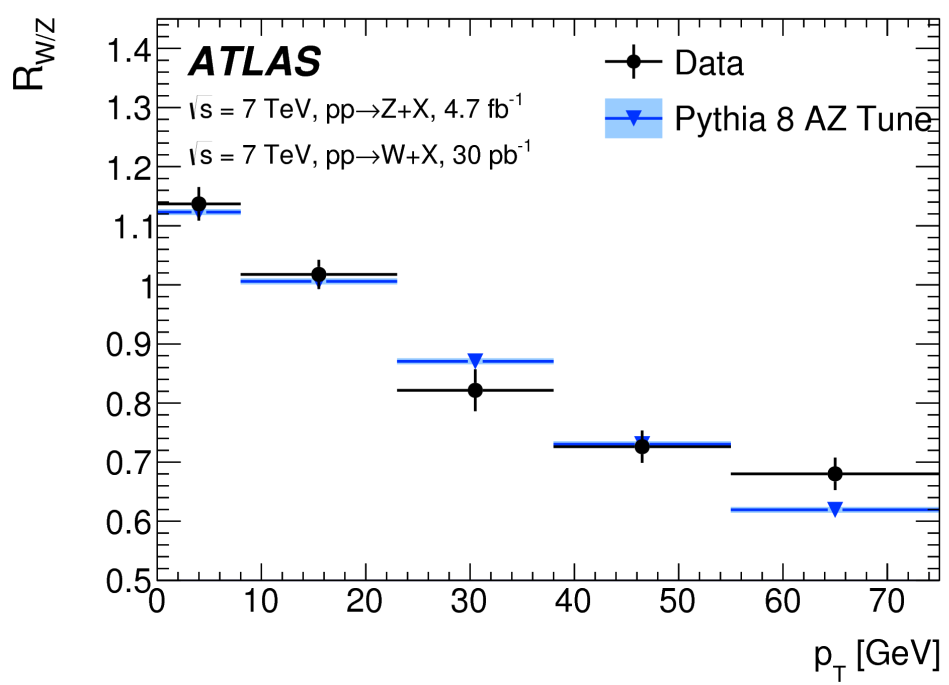

- The ratio of the W and Z p_T distributions has been measured – it shows that the **extrapolation from Z to W p_T works ok**

Summary of physics modelling uncertainties

QCD

W-boson charge	W^+		W^-		Combined	
Kinematic distribution	p_T^ℓ	m_T	p_T^ℓ	m_T	p_T^ℓ	m_T
δm_W [MeV]						
Fixed-order PDF uncertainty	13.1	14.9	12.0	14.2	8.0	8.7
AZ tune	3.0	3.4	3.0	3.4	3.0	3.4
Charm-quark mass	1.2	1.5	1.2	1.5	1.2	1.5
Parton shower μ_F with heavy-flavour decorrelation	5.0	6.9	5.0	6.9	5.0	6.9
Parton shower PDF uncertainty	3.6	4.0	2.6	2.4	1.0	1.6
Angular coefficients	5.8	5.3	5.8	5.3	5.8	5.3
Total	15.9	18.1	14.8	17.2	11.6	12.9

EW

Decay channel	$W \to e\nu$		$W \to \mu\nu$	
Kinematic distribution	p_T^ℓ	m_T	p_T^ℓ	m_T
δm_W [MeV]				
FSR (real)	< 0.1	< 0.1	< 0.1	< 0.1
Pure weak and IFI corrections	3.3	2.5	3.5	2.5
FSR (pair production)	3.6	0.8	4.4	0.8
Total	4.9	2.6	5.6	2.6

- Fixed-order **PDF uncertainties are dominant**:
  - PDF variations of CT10nnlo applied simultaneously to y_W, A_i and p_T^W distributions
  - Envelope taken from CT14 and MMHT14 ~ 3.8 MeV
- PDF uncertainties very similar between p_T^l and m_T but strongly anti-correlated between W+ and W-

Recoil calibration

- The **recoil $\vec{u}_T$** is the vector sum of the transverse energy of all the calorimeter clusters → a **measure of p_T^W**

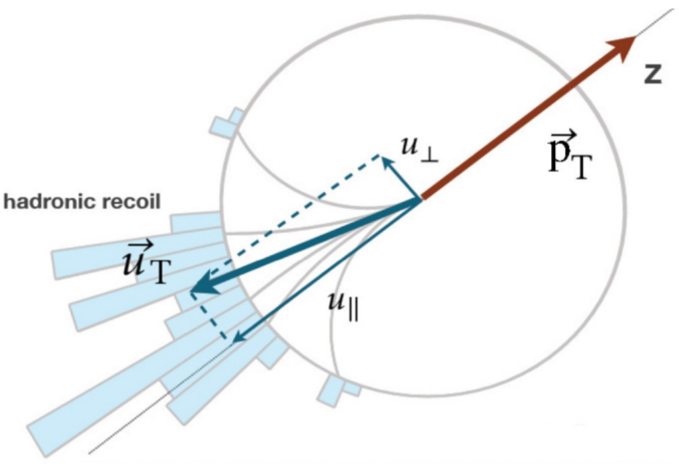

- Calibration steps:
  - Correct pile-up multiplicity in MC to match the data
  - Correct for residual differences in the $\sum E_T$ distribution
  - Derive scale and resolution corrections from the p_T balance in Z events

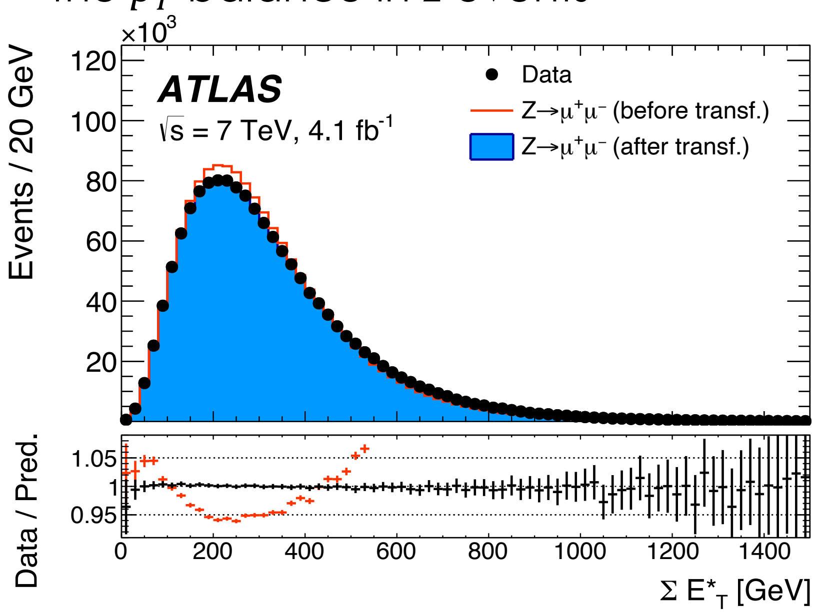

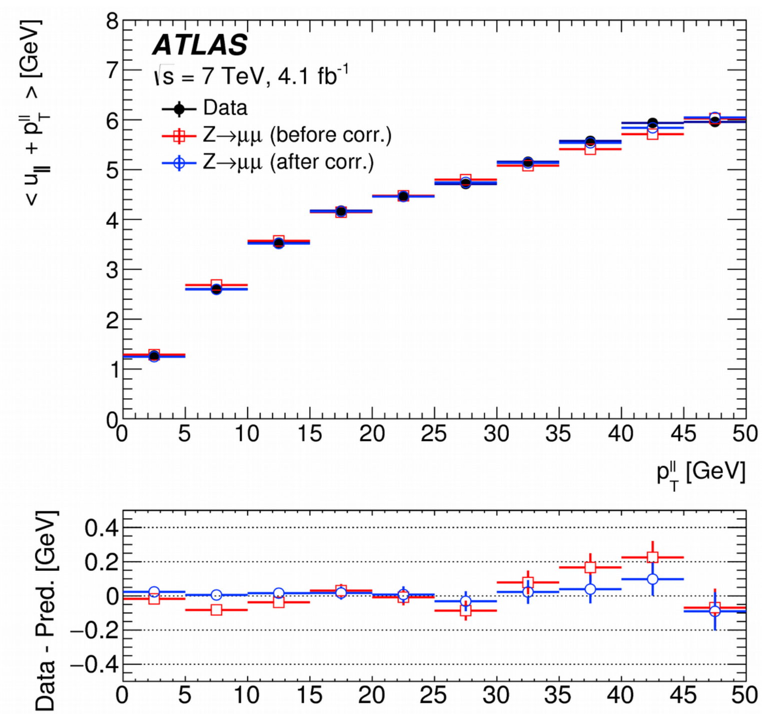

Consistency of the results

- The consistency of the results was checked in different categories, but also in different pile-up and u_T bins

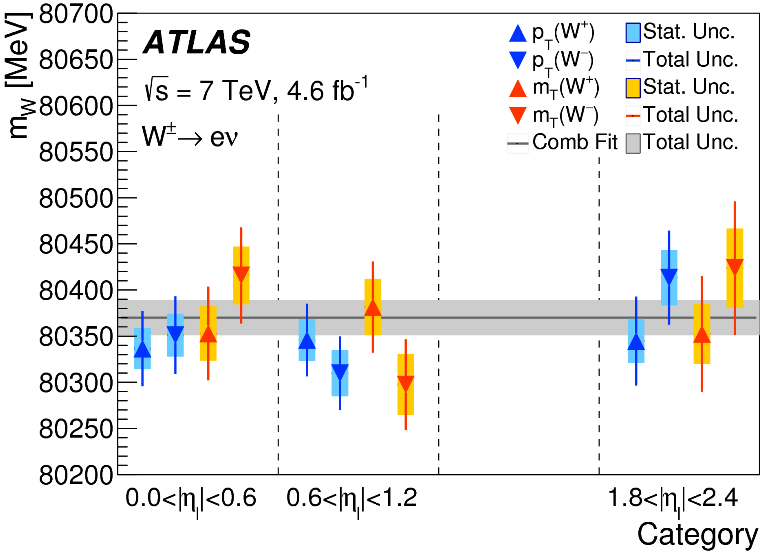

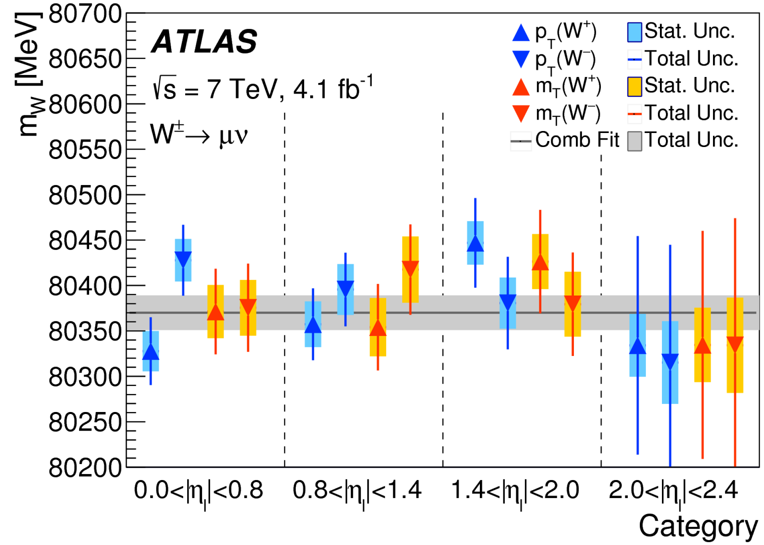

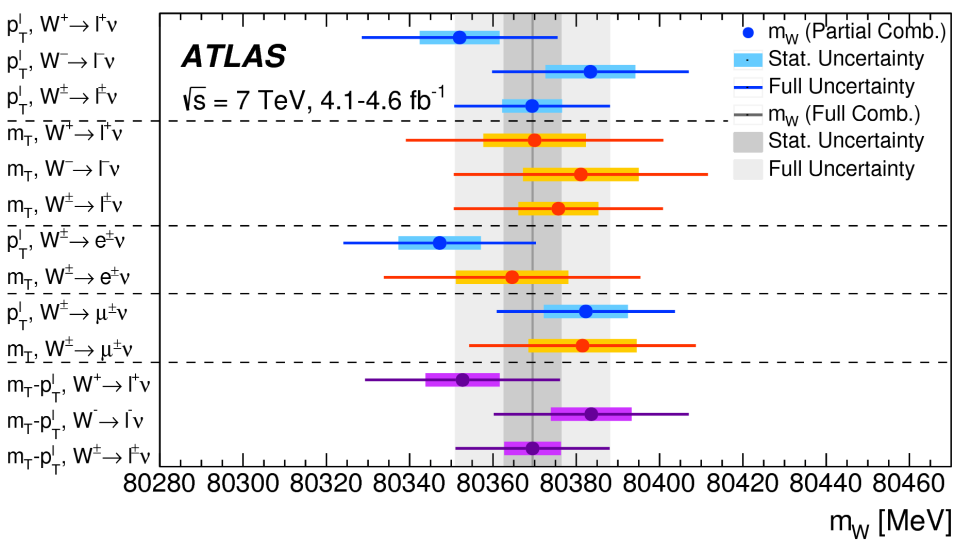

Crucial validation

Fitting ranges:
$32 < p_T^l < 45$ GeV
$66 < m_T < 99$ GeV

W mass results

$$m_W = 80369.5 \pm 6.8\,\text{MeV}(\text{stat.}) \pm 10.6\,\text{MeV}(\text{exp. syst.}) \pm 13.6\,\text{MeV}(\text{mod. syst.})$$
$$= 80369.5 \pm 18.5\,\text{MeV},$$

Combined categories	Value [MeV]	Stat. Unc.	Muon Unc.	Elec. Unc.	Recoil Unc.	Bckg. Unc.	QCD Unc.	EWK Unc.	PDF Unc.	Total Unc.	χ^2/dof of Comb.
m_T-p_T^ℓ, $W^\pm$, e-μ	80369.5	6.8	6.6	6.4	2.9	4.5	8.3	5.5	9.2	18.5	29/27

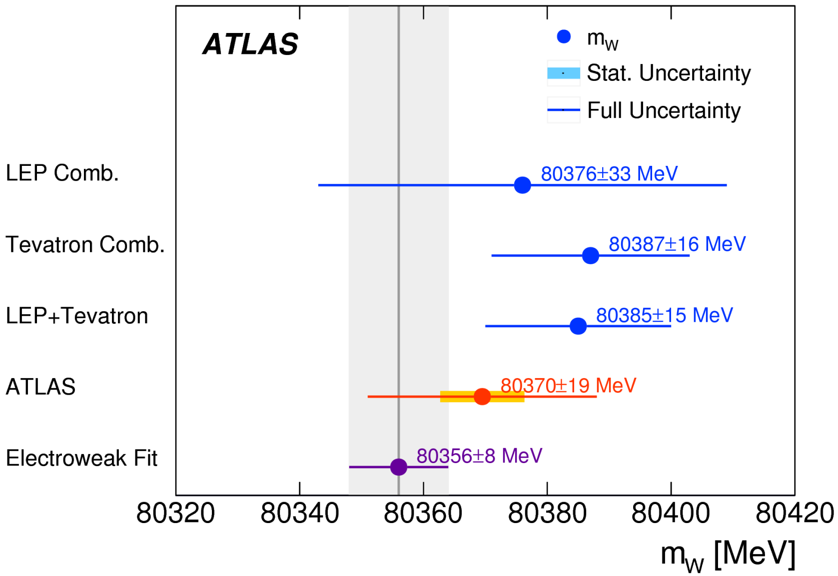

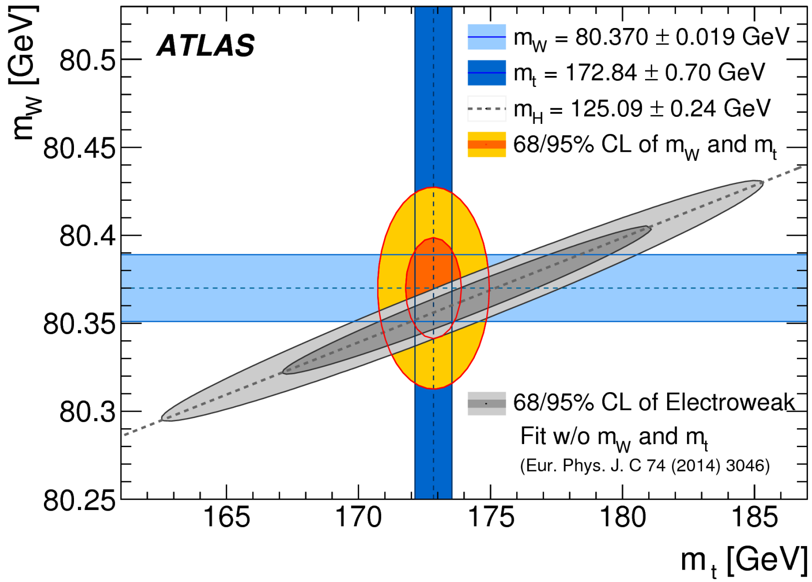

- **The result is consistent with the SM expectation**, compatible with world average and competitive in precision with the CDF and D0 measurements

Prospects for improvements

$$m_W = 80369.5 \pm 6.8\ \text{MeV(stat.)} \pm 10.6\ \text{MeV(exp. syst.)} \pm 13.6\ \text{MeV(mod. syst.)}$$

- **Stat. uncertainty:** add more data available
- **Exp. uncertainty:** improve the experimental precision – calibration and reconstruction
- **Theory-related uncertainties:** reduce PDFs and modelling uncertainties by adding more information from auxiliary measurements

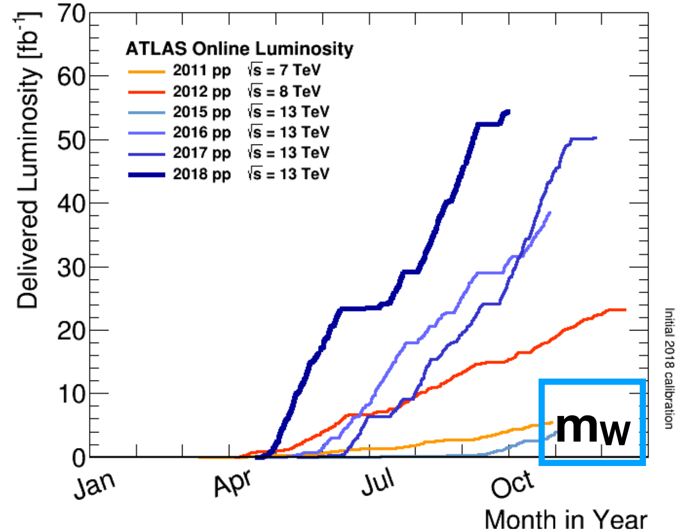

In November 2017 special low pile-up runs of a few days:

- ~250 pb^{-1} @5 TeV $\mu = 0.5 \sim 4.0$
- ~150 pb^{-1} @13 TeV $\mu = 2.0$ (levelled)

In 2018: ~190 pb^{-1} @13 TeV $\mu = 2.0$ (levelled)

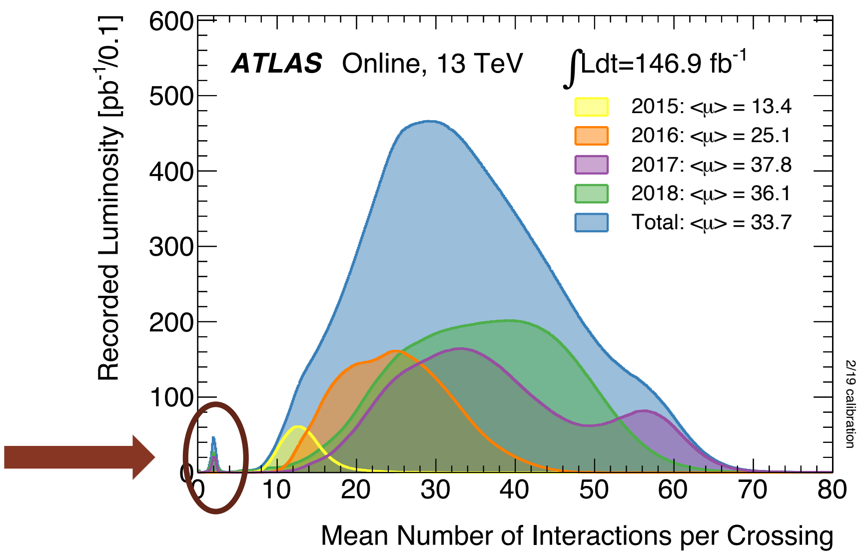

Low μ runs

ATLAS-PUB-2017-021

- The recoil resolution degrades with higher pileup → fully dominated by p_T lepton
- Increase sensitivity from m_T
- Direct p_T^W measurement → use information to reduce p_T modelling uncertainties also in high pile-up runs
- Ideally low μ run in **Run 3** as well! **0.5-1 fb^{-1} at $<\mu>\sim 2$** highly beneficial
- ~300 pb^{-1} already collected at $<\mu>\sim 1$ by ATLAS and CMS can provide a new ~1% measurement of p_T^W and significantly reduce the associated uncertainty

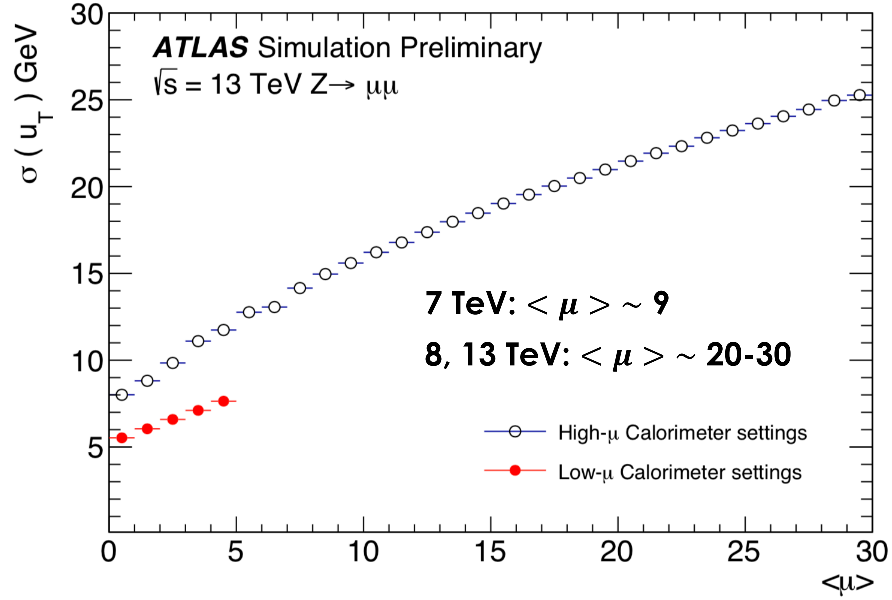

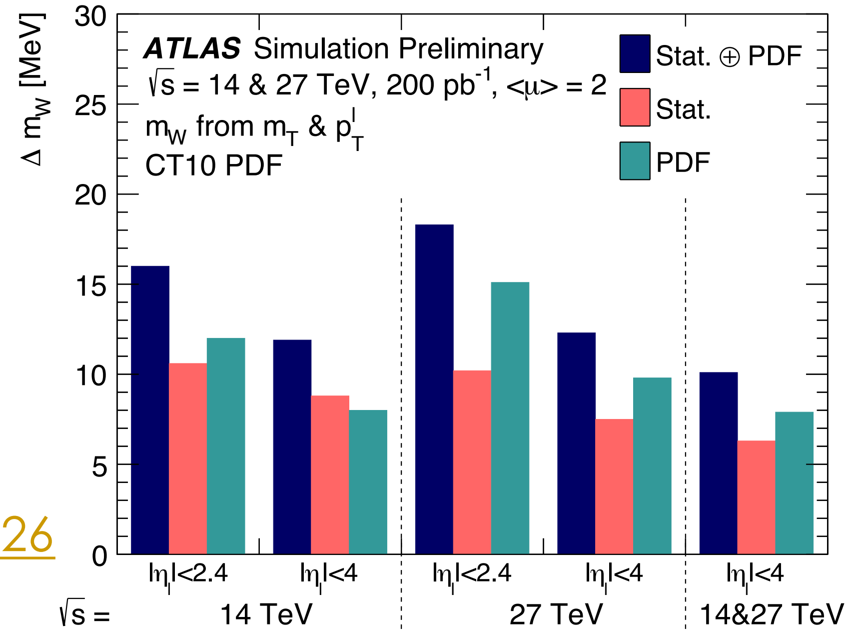

ATLAS-PUB-2018-026

Implications on m_W measurement

- Reduction of PDF uncertainties crucial for SM precision measurements → one of the largest systematic on m_W comes from PDFs
- The potential of the lepton-charge (**A_W**) and the forward-backward asymmetries (**A_{FB}**) in constraining PDFs has been investigated - Nuclear Physics B 968 (2021) 115444, JHEP 10 (2019) 176
- Combination of A_{FB} and A_W 300 (3000) fb^{-1} reduces PDF uncertainty **28%** (**46%**)

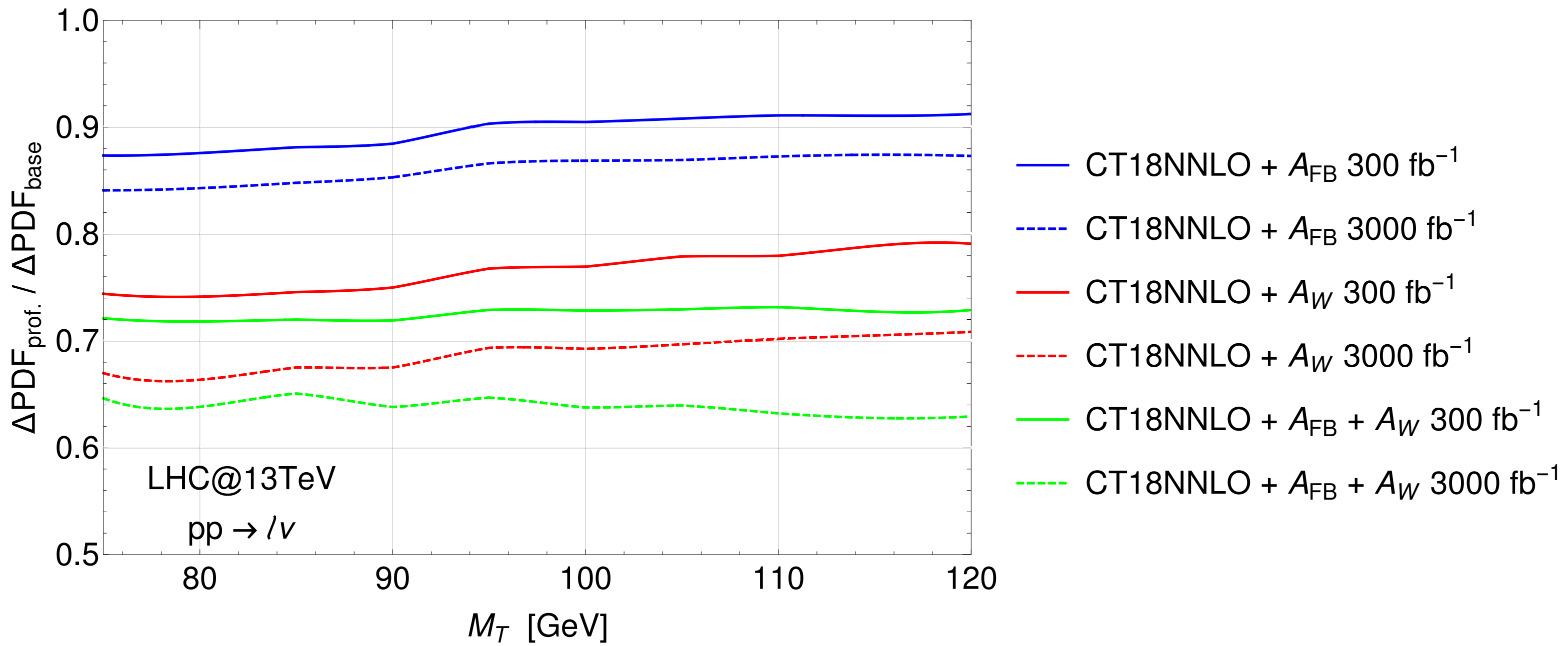

- **Caveat:** assessing the improvement on m_W requires a refined analysis of normalized distributions, where reduction of uncertainty is far more moderate

Conclusion and perspectives

- The first LHC measurement of **m_W = 80370 $\pm$ 19 MeV** - EPJC 78 (2018) 110
- The central value is consistent with the SM prediction and with the current world average value
- 7 TeV re-analysis currently ongoing in ATLAS
- More data are available with the 8 and 13 TeV data sets which can be used to improve the analysis and to further constrain the PDFs
- Experimentally, with the increase of the statistics in Z sample, most of the calibration uncertainties can be reduced
- More work is needed on the recoil with the increasing pileup – **low pile-up runs** needed
- **The measurement is dominated by theoretical modelling uncertainties → ** *a fully consistent model within one simulation tool* is needed
- Simultaneous fit to all the A_i and dedicated analysis on m_W and $\sin^2 \theta_W$ determination ongoing… STAY TUNED!

THANKS FOR YOUR ATTENTION!

ANY QUESTIONS?

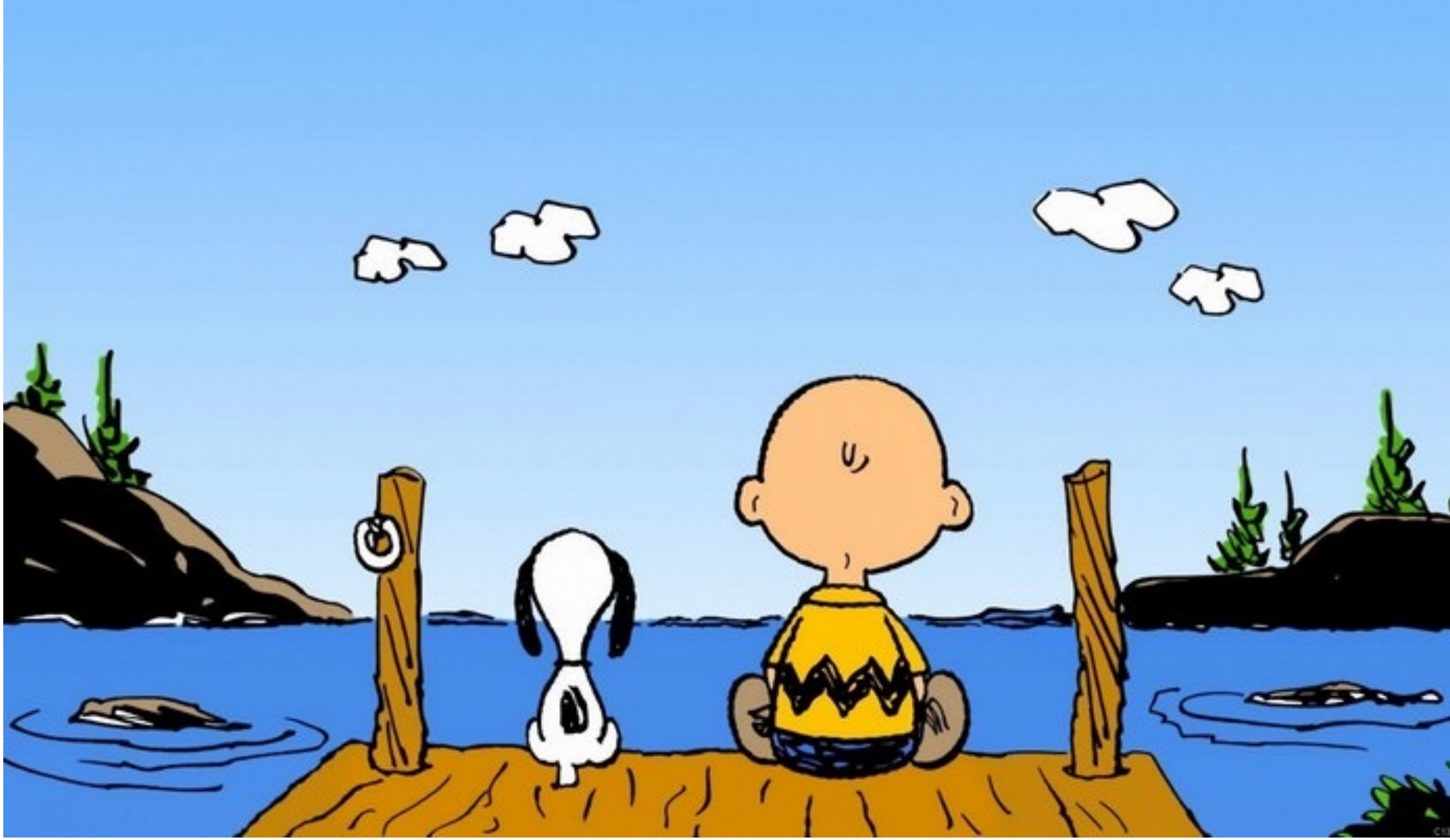

Backup Slides

Motivation

- The global fit of EW observables dominated by the m_W measurement

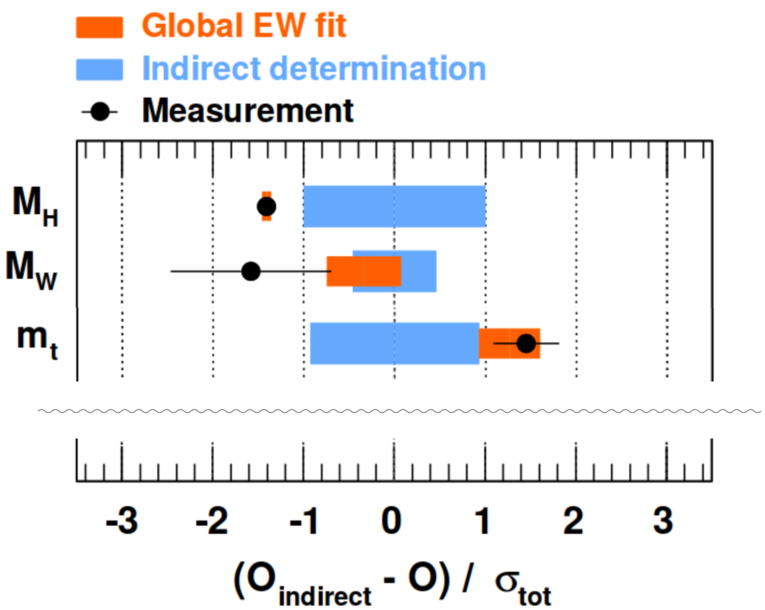

	Measurement	SM Prediction (*)
m_H	125.09 ± 0.24	100.6 ± 23.6
m_t	173.1 ± 0.6	176.1 ± 2.2
m_W	80.379 ± 0.012	80.360 ± 0.007

(*) 1710.05402

- The measurements of the Higgs and top-quark mass are currently more precise than their indirect determination from the the global fit of EW observables → improving precision will not increase sensitivity to new physics

- Indirect determination of m_W (± 7 MeV) is more precise than experimental measurements → **call for a δm_W^{exp} ~ 5 MeV**

- The **W mass** is nowadays the **crucial measurement to improve sensitivity of the global EW fits to new physics**

MSSM constraints from the W mass

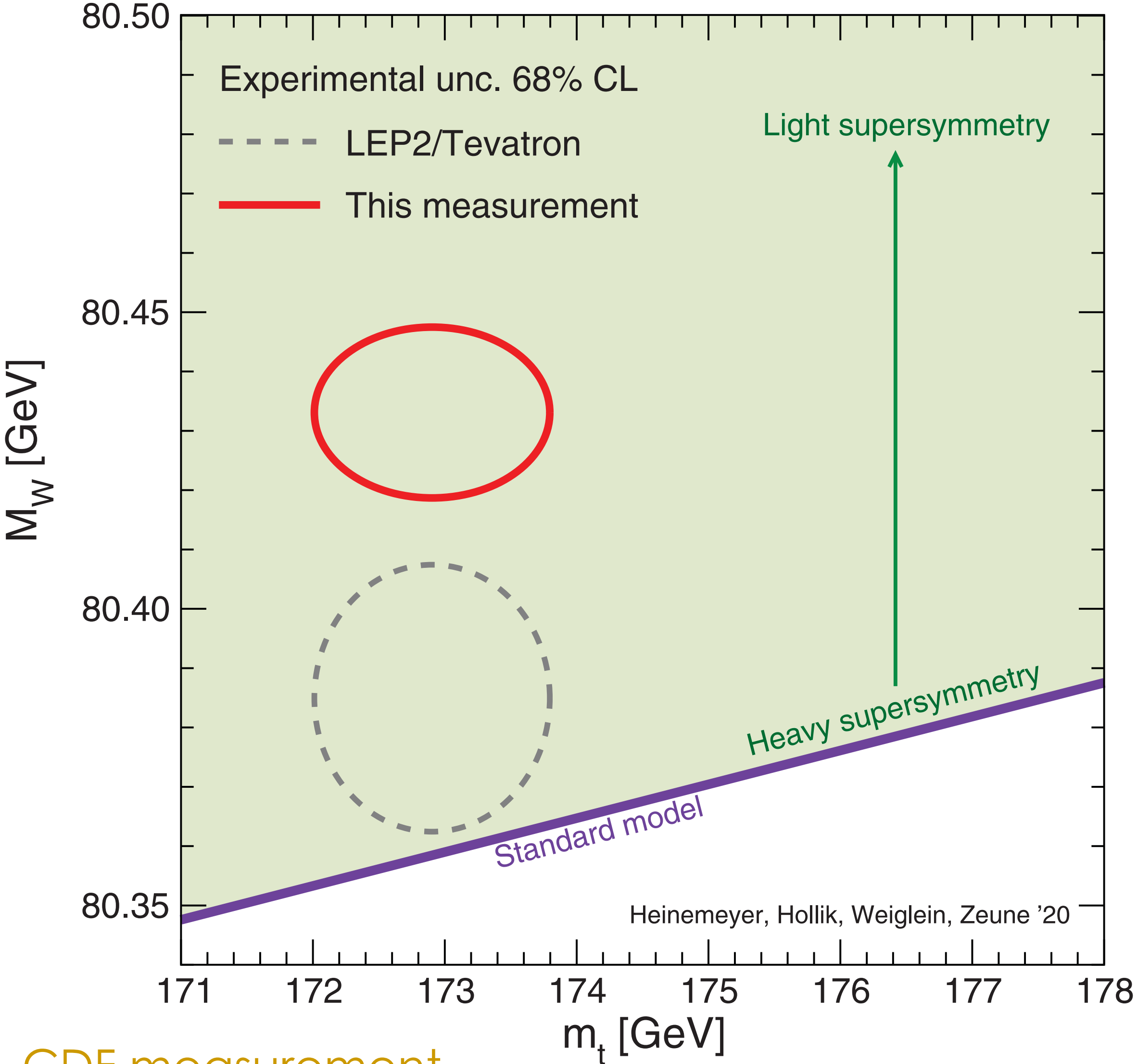

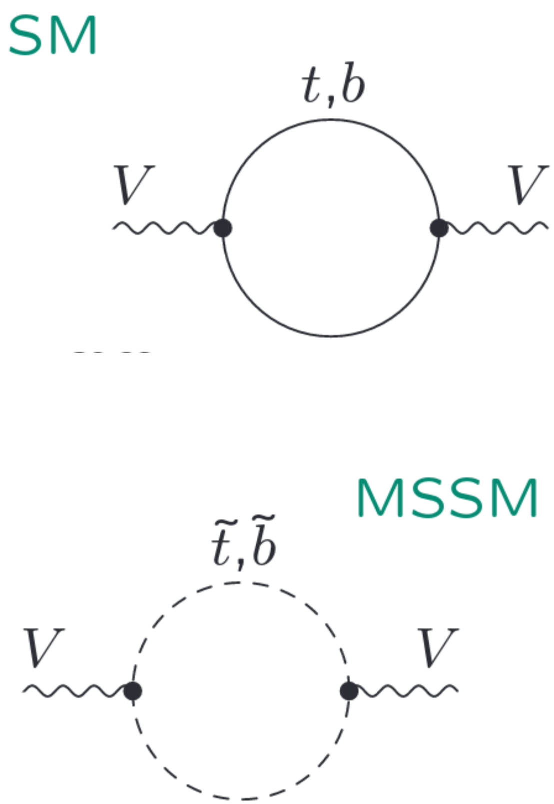

CDF measurement

Selection cuts

- Lepton selection:
  - Isolated muons (track-based), $|\eta| < 2.4$
  - Isolated electrons (track+calorimeter-based), tight identified, $0.0 < |\eta| < 1.2$ and $1.8 < |\eta| < 2.4$

- Kinematic requirements:
  - $p_T^l > 30$ GeV
  - $m_T > 60$ GeV
  - MET > 30 GeV
  - Recoil $u_T < 30$ GeV

~6/8M events observed in the electron/muon channel

$\lvert\eta_\ell\rvert$ range	0–0.8	0.8–1.4	1.4–2.0	2.0–2.4	Inclusive
$W^+ \to \mu^+\nu$	1 283 332	1 063 131	1 377 773	885 582	4 609 818
$W^- \to \mu^-\bar{\nu}$	1 001 592	769 876	916 163	547 329	3 234 960
$\lvert\eta_\ell\rvert$ range	0–0.6	0.6–1.2		1.8–2.4	Inclusive
$W^+ \to e^+\nu$	1 233 960	1 207 136		956 620	3 397 716
$W^- \to e^-\bar{\nu}$	969 170	908 327		610 028	2 487 525

Template fit

- **Template fit approach:** compute the p_T^l and m_T distributions for different assumed values of m_W → χ^2 minimisation gives the best fit template

- Predictions for different m_W values are obtained by reweighting the boson invariant mass distribution according to the Breit-Wigner parametrisation

$$\frac{d\sigma}{dm} \propto \frac{m^2}{(m^2 - m_V^2)^2 + m^4\Gamma_V^2/m_V^2}$$

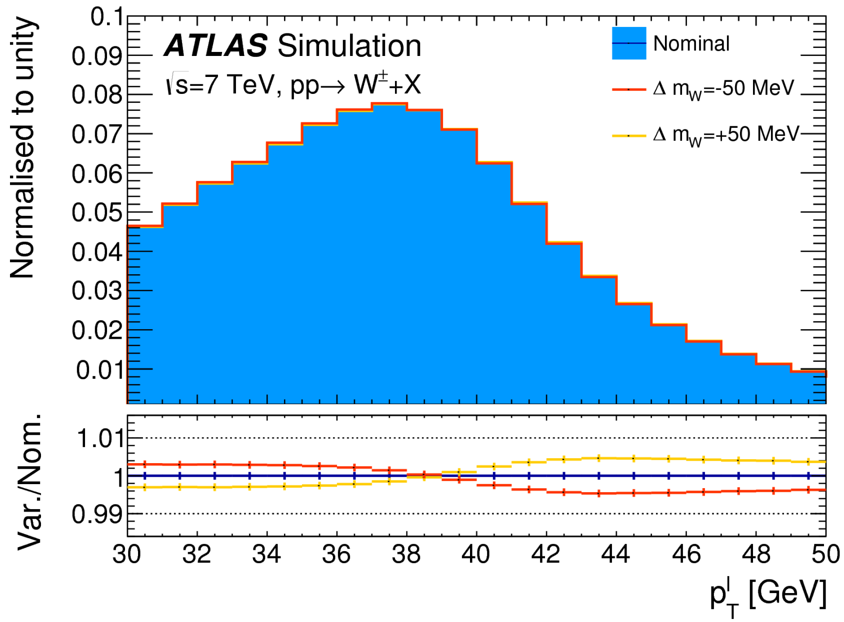

p_T^l has a Jacobin edge at $m_W/2$

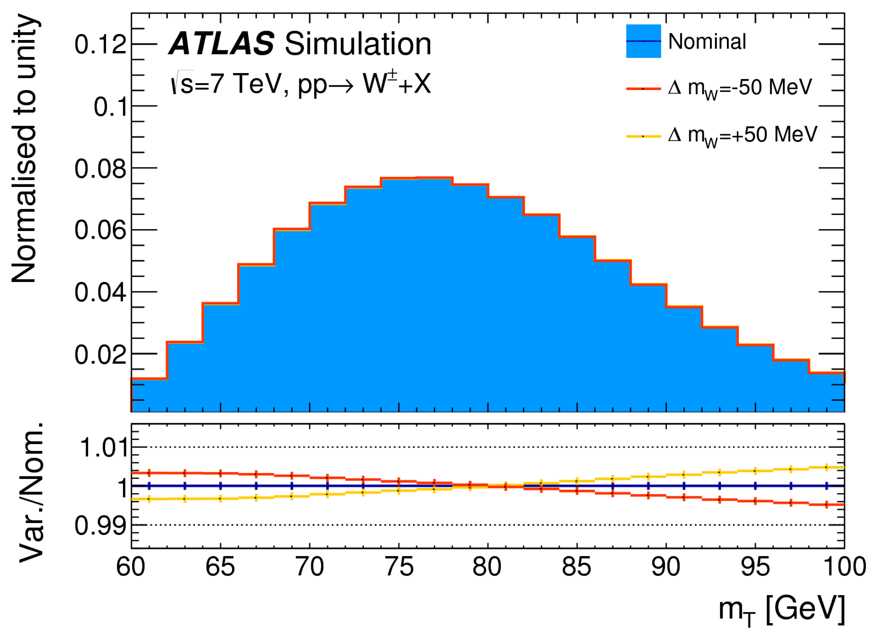

m_T has a Jacobin edge at m_W

Backgrounds

- Electroweak and top-quark are determined from simulation
- Data-driven multijet estimate:
  - Define background-dominated fit region with relaxed cuts of the event selection
  - Template fits in these regions to 3 observables: p_T^{miss}, m_T and p_T^l/m_T
  - Control regions obtained by inverting the lepton isolation requirements

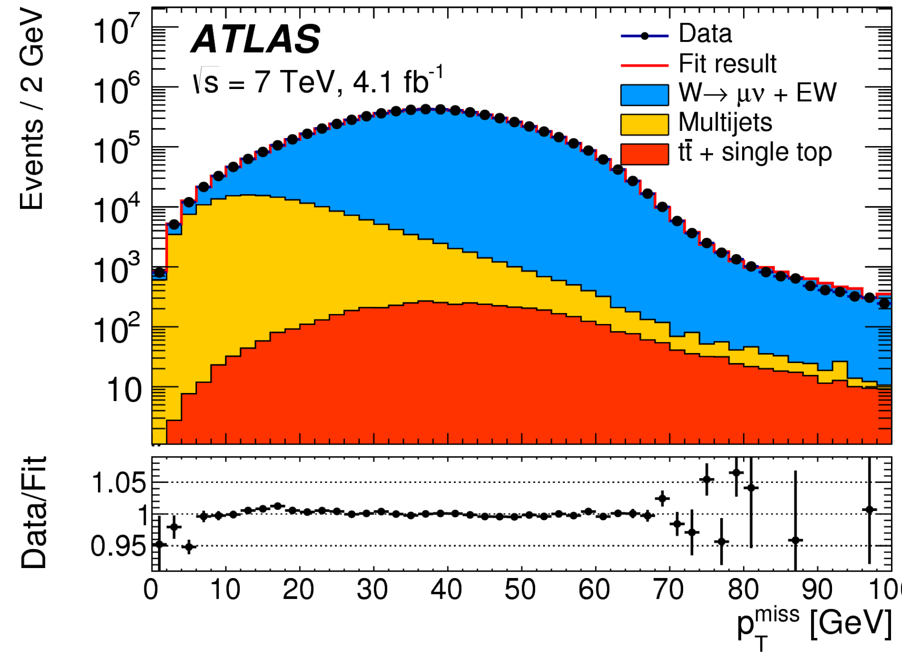

$W \to \mu\nu$						
Category	$W \to \tau\nu$	$Z \to \mu\mu$	$Z \to \tau\tau$	Top	Dibosons	Multijet
$W^{\pm}$ $0.0 < \lvert\eta\rvert < 0.8$	1.04	2.83	0.12	0.16	0.08	0.72
$W^{\pm}$ $0.8 < \lvert\eta\rvert < 1.4$	1.01	4.44	0.11	0.12	0.07	0.57
$W^{\pm}$ $1.4 < \lvert\eta\rvert < 2.0$	0.99	6.78	0.11	0.07	0.06	0.51
$W^{\pm}$ $2.0 < \lvert\eta\rvert < 2.4$	1.00	8.50	0.10	0.04	0.05	0.50
$W^{\pm}$ all η bins	1.01	5.41	0.11	0.10	0.06	0.58
W^{+} all η bins	0.99	4.80	0.10	0.09	0.06	0.51
W^{-} all η bins	1.04	6.28	0.14	0.12	0.08	0.68

$W \to e\nu$						
Category	$W \to \tau\nu$	$Z \to ee$	$Z \to \tau\tau$	Top	Dibosons	Multijet
$W^{\pm}$ $0.0 < \lvert\eta\rvert < 0.6$	1.02	3.34	0.13	0.15	0.08	0.59
$W^{\pm}$ $0.6 < \lvert\eta\rvert < 1.2$	1.00	3.48	0.12	0.13	0.08	0.76
$W^{\pm}$ $1.8 < \lvert\eta\rvert < 2.4$	0.97	3.23	0.11	0.05	0.05	1.74
$W^{\pm}$ all η bins	1.00	3.37	0.12	0.12	0.07	1.00
W^{+} all η bins	0.98	2.92	0.10	0.11	0.06	0.84
W^{-} all η bins	1.04	3.98	0.14	0.13	0.08	1.21

Kinematic distribution	p_T^ℓ				m_T			
Decay channel	$W \to e\nu$		$W \to \mu\nu$		$W \to e\nu$		$W \to \mu\nu$	
W-boson charge	W^+	W^-	W^+	W^-	W^+	W^-	W^+	W^-
δm_W [MeV]								
$W \to \tau\nu$ (fraction, shape)	0.1	0.1	0.1	0.2	0.1	0.2	0.1	0.3
$Z \to ee$ (fraction, shape)	3.3	4.8	–	–	4.3	6.4	–	–
$Z \to \mu\mu$ (fraction, shape)	–	–	3.5	4.5	–	–	4.3	5.2
$Z \to \tau\tau$ (fraction, shape)	0.1	0.1	0.1	0.2	0.1	0.2	0.1	0.3
WW, WZ, ZZ (fraction)	0.1	0.1	0.1	0.1	0.4	0.4	0.3	0.4
Top (fraction)	0.1	0.1	0.1	0.1	0.3	0.3	0.3	0.3
Multijet (fraction)	3.2	3.6	1.8	2.4	8.1	8.6	3.7	4.6
Multijet (shape)	3.8	3.1	1.6	1.5	8.6	8.0	2.5	2.4
Total	6.0	6.8	4.3	5.3	12.6	13.4	6.2	7.4

Multijet background estimate

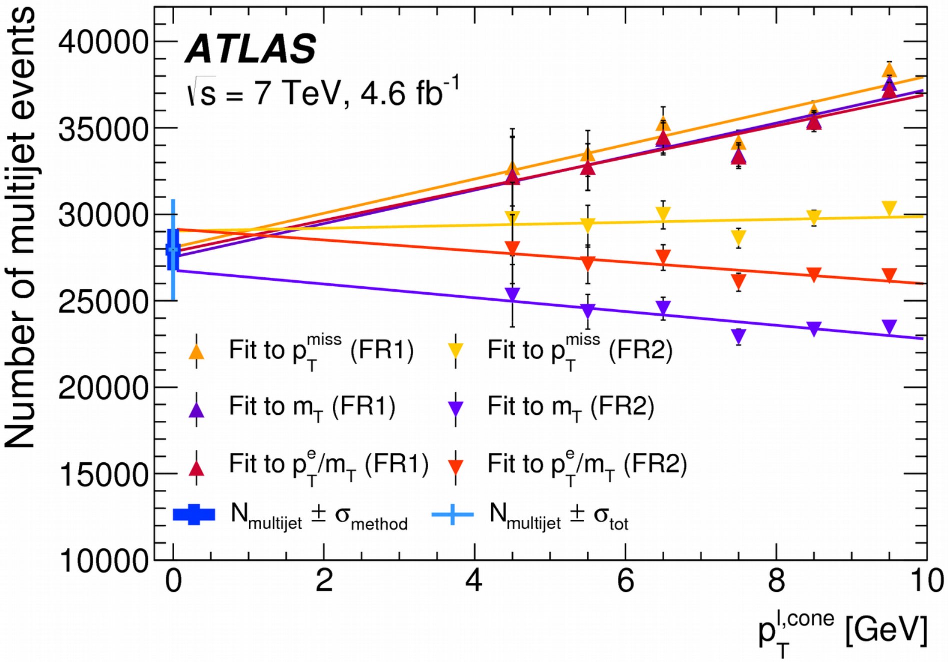

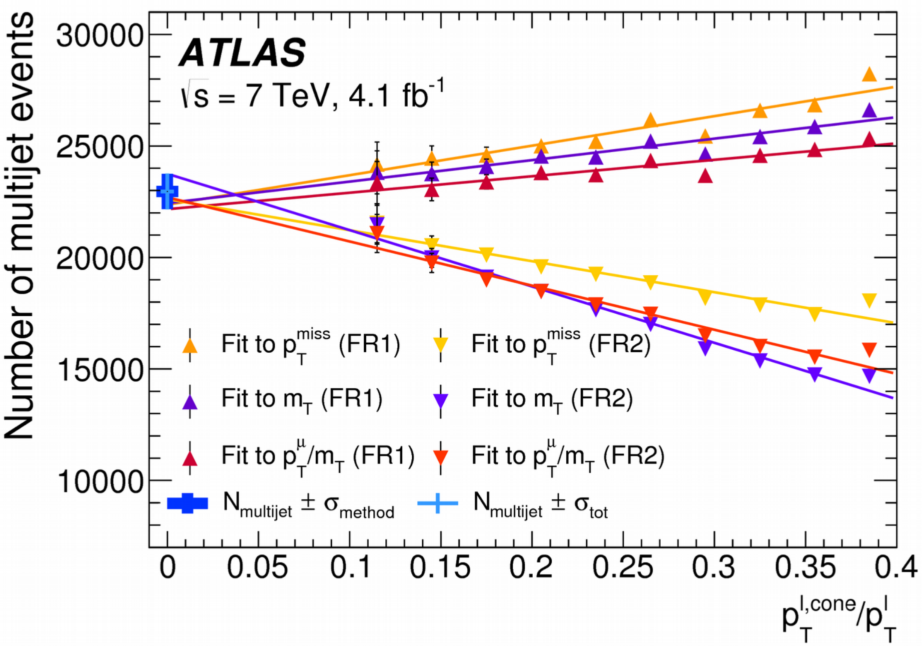

- Novel technique for the multijet background estimation
- The multijet background is determined with template fits, and by extrapolation of the lepton isolation to the signal region
- Both normalisation and shape are extrapolated

Drell-Yan ancillary measurements

$$\frac{d\sigma}{dp_1\, dp_2} = \left[\frac{d\sigma(m)}{dm}\right]\left[\frac{d\sigma(y)}{dy}\right]\left[\frac{d\sigma(p_T, y)}{dp_T\, dy}\left(\frac{d\sigma(y)}{dy}\right)^{-1}\right]\left[(1+\cos^2\theta) + \sum_{i=0}^{7} A_i(p_T, y) P_i(\cos\theta, \phi)\right]$$

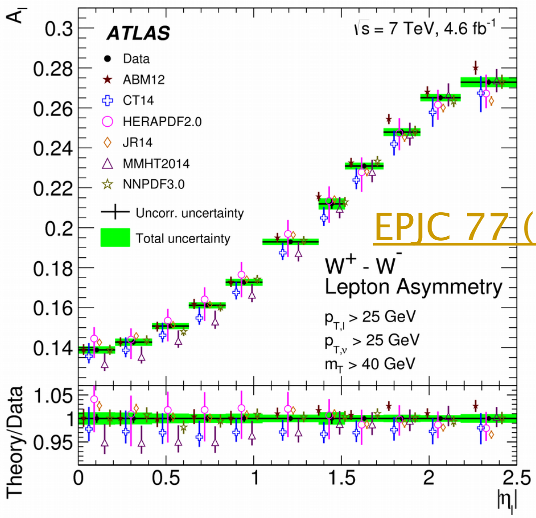

EPJC 77 (2017) 367

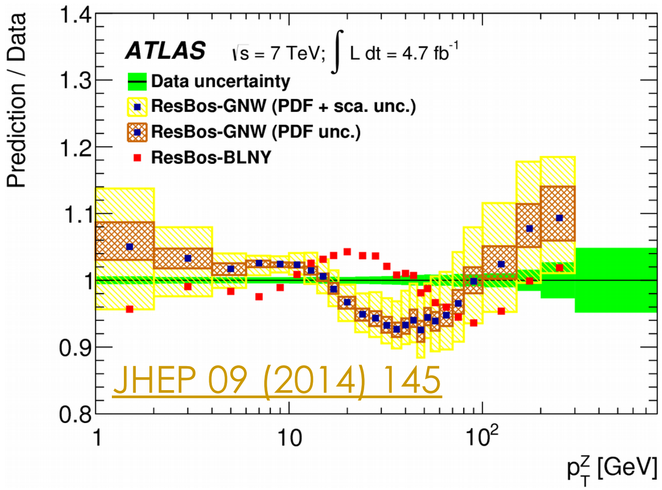

JHEP 09 (2014) 145

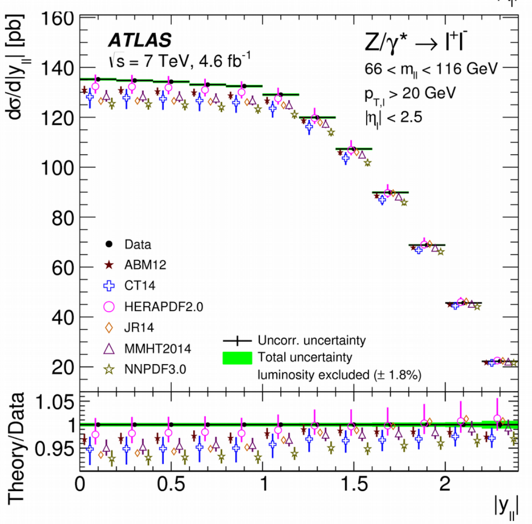

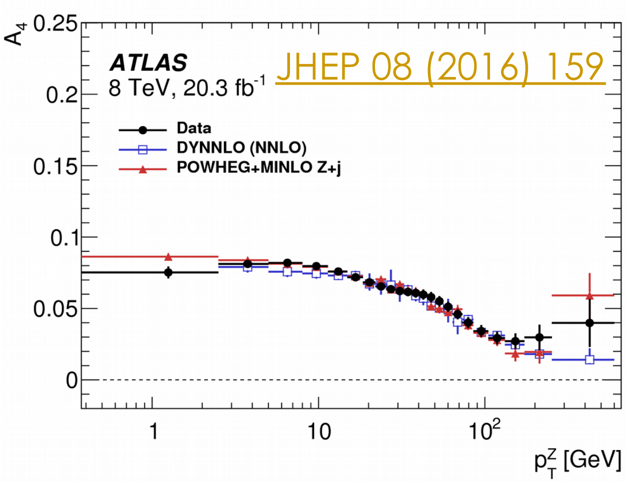

JHEP 08 (2016) 159

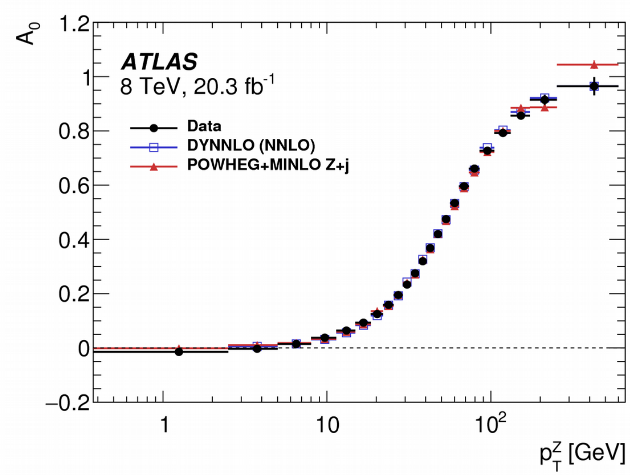

Muon calibration

- Muon identification using combined ID+MS tracks — EPJC 74 (2014) 3130
- Momentum measurement from ID only → simplifies calibration, some loss in resolution
- Parametrisation of momentum corrections:

$$p_{\mathrm{T}}^{\mathrm{corr}} = p_{\mathrm{T}}^{\mathrm{MC}} \times \frac{1+\alpha(\eta,\phi)}{1+q\cdot\delta(\eta,\phi)\cdot p_{\mathrm{T}}^{\mathrm{MC}}}\left[1+\beta_{\mathrm{curv}}(\eta)\cdot G(0,1)\cdot p_{\mathrm{T}}^{\mathrm{MC}}\right]$$

- α = radial bias (scale), β = resolution correction and δ = sagitta bias

$\lvert\eta_\ell\rvert$ range / Kinematic distribution	Combined p_{T}^{ℓ}	Combined m_{T}
δm_W [MeV]		
Momentum scale	8.4	8.8
Momentum resolution	1.0	1.2
Sagitta bias	0.6	0.6
Reconstruction and isolation efficiencies	2.7	2.2
Trigger efficiency	4.1	3.2
Total	9.8	9.7

Charge-dependent corrections

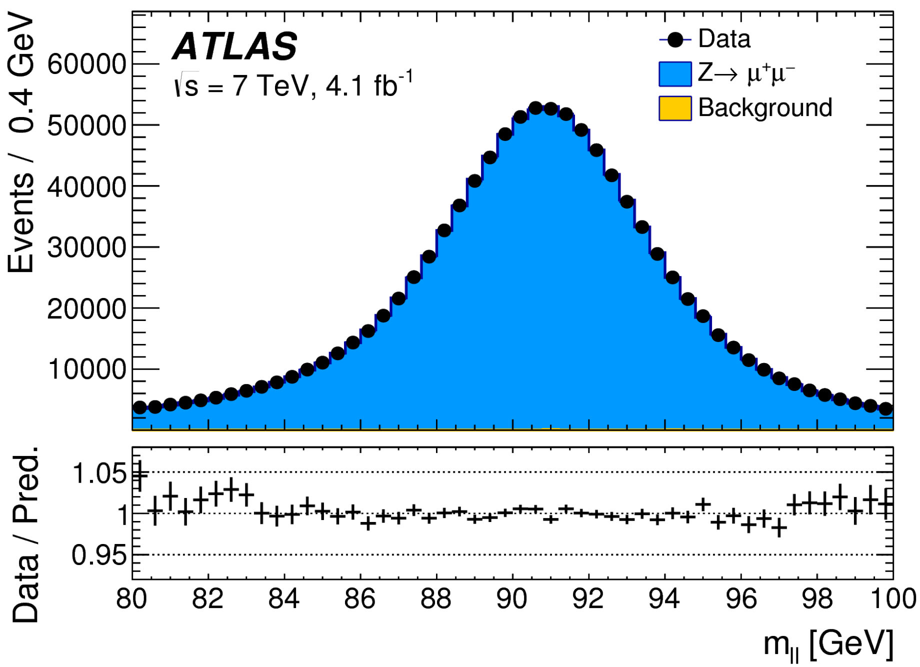

Electron calibration

EPJC 74 (2014) 3071

- Electron measurement: energy from the EM calorimeter, η and ϕ from the ID
- Scale and resolution corrections derived from the Z → e^+e^- line shape
- ϕ – dependent corrections are important for the Z to W extrapolation
- The p_T^{miss} requirement (which is only only used for W events) induces a ϕ asymmetry in the selected W events distribution

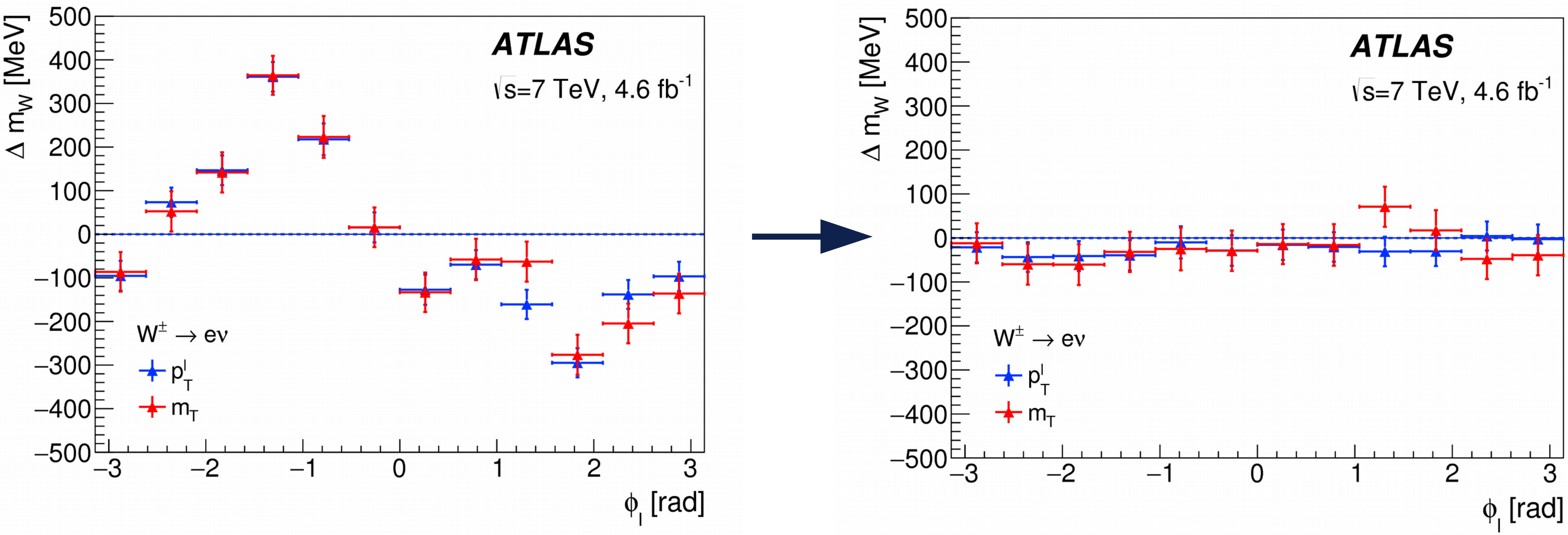

Electron calibration

EPJC 74 (2014) 3071

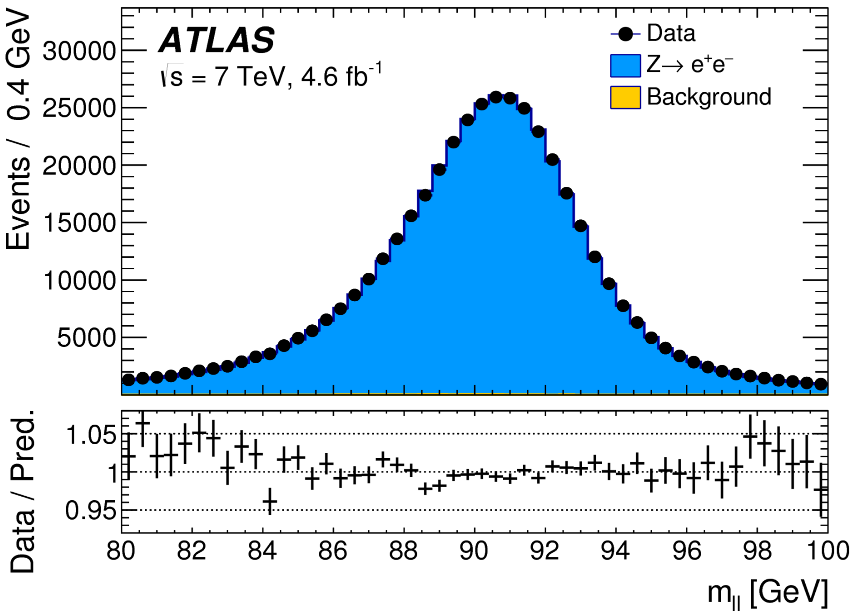

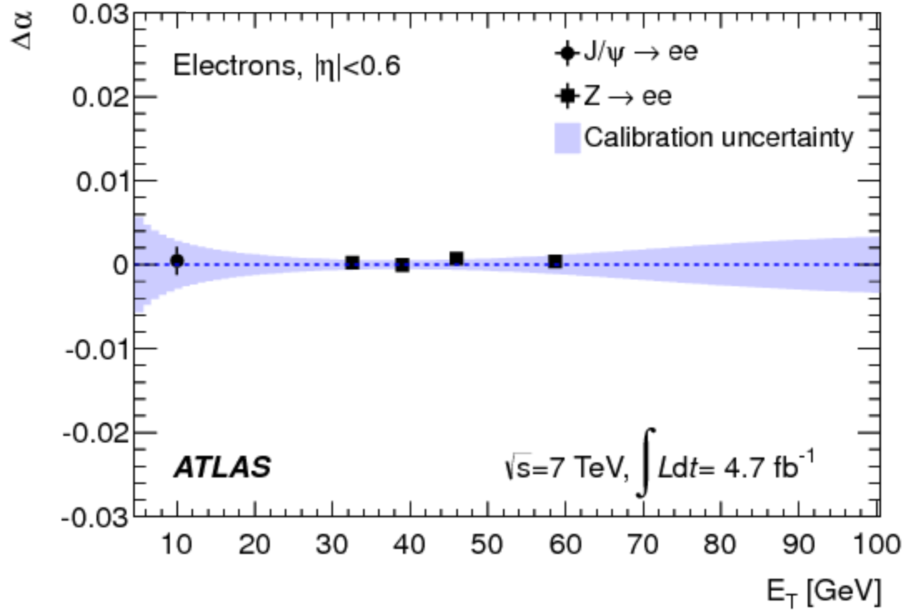

➢ Exclude bin $1.2 < |\eta| < 1.82$ – largest amount of passive material

$\|\eta_\ell\|$ range	[0.0, 0.6]		[0.6, 1.2]		[1.82, 2.4]		Combined	
Kinematic distribution	p_T^ℓ	m_T	p_T^ℓ	m_T	p_T^ℓ	m_T	p_T^ℓ	m_T
δm_W [MeV]								
Energy scale	10.4	10.3	10.8	10.1	16.1	17.1	8.1	8.0
Energy resolution	5.0	6.0	7.3	6.7	10.4	15.5	3.5	5.5
Energy linearity	2.2	4.2	5.8	8.9	8.6	10.6	3.4	5.5
Energy tails	2.3	3.3	2.3	3.3	2.3	3.3	2.3	3.3
Reconstruction efficiency	10.5	8.8	9.9	7.8	14.5	11.0	7.2	6.0
Identification efficiency	10.4	7.7	11.7	8.8	16.7	12.1	7.3	5.6
Trigger and isolation efficiencies	0.2	0.5	0.3	0.5	2.0	2.2	0.8	0.9
Charge mismeasurement	0.2	0.2	0.2	0.2	1.5	1.5	0.1	0.1
Total	19.0	17.5	21.1	19.4	30.7	30.5	14.2	14.3

Z mass measurement

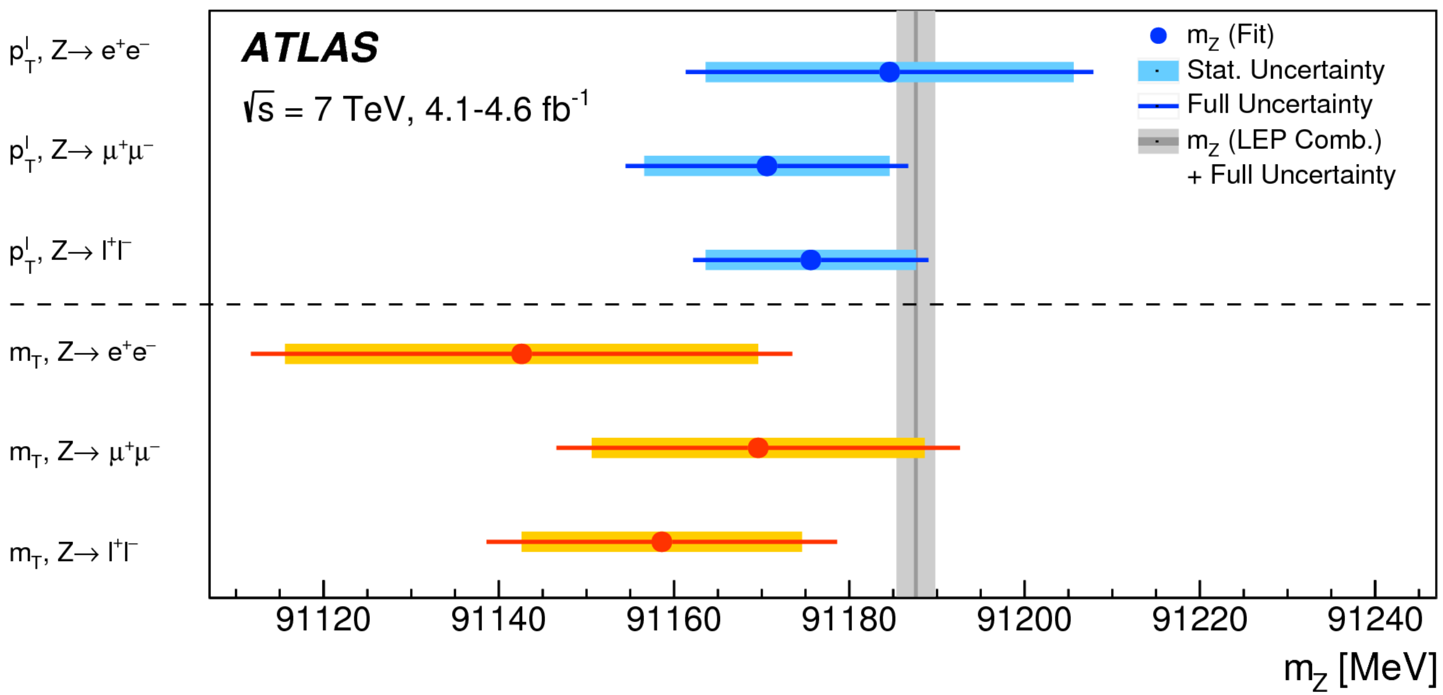

Lepton charge Distribution	ℓ^+ p_T^ℓ	ℓ^+ m_T	ℓ^- p_T^ℓ	ℓ^- m_T	Combined p_T^ℓ	Combined m_T
Δm_Z [MeV]			41			
$Z \rightarrow ee$	$13 \pm 31 \pm 10$	$-93 \pm 38 \pm 15$	$-20 \pm 31 \pm 10$	$4 \pm 38 \pm 15$	$-3 \pm 21 \pm 10$	$-45 \pm 27 \pm 15$
$Z \rightarrow \mu\mu$	$1 \pm 22 \pm 8$	$-35 \pm 28 \pm 13$	$-36 \pm 22 \pm 8$	$-1 \pm 27 \pm 13$	$-17 \pm 14 \pm 8$	$-18 \pm 19 \pm 13$
Combined	$5 \pm 18 \pm 6$	$-58 \pm 23 \pm 12$	$-31 \pm 18 \pm 6$	$1 \pm 22 \pm 12$	$-12 \pm 12 \pm 6$	$-29 \pm 16 \pm 12$

Results are consistent with the combined LEP value of m_Z within experimental uncertainties

W transverse momentum

- The Pythia8 AZ tune is fixed by the p_T^Z data – extrapolate to W considering relative variations of the W and Z p_T distributions

- Resummed predictions (DYRES, ResBos, CuTe) and Powheg MiNLO + Pythia8 were tried but they predict harder p_T^W spectrum for a given p_T^Z spectrum

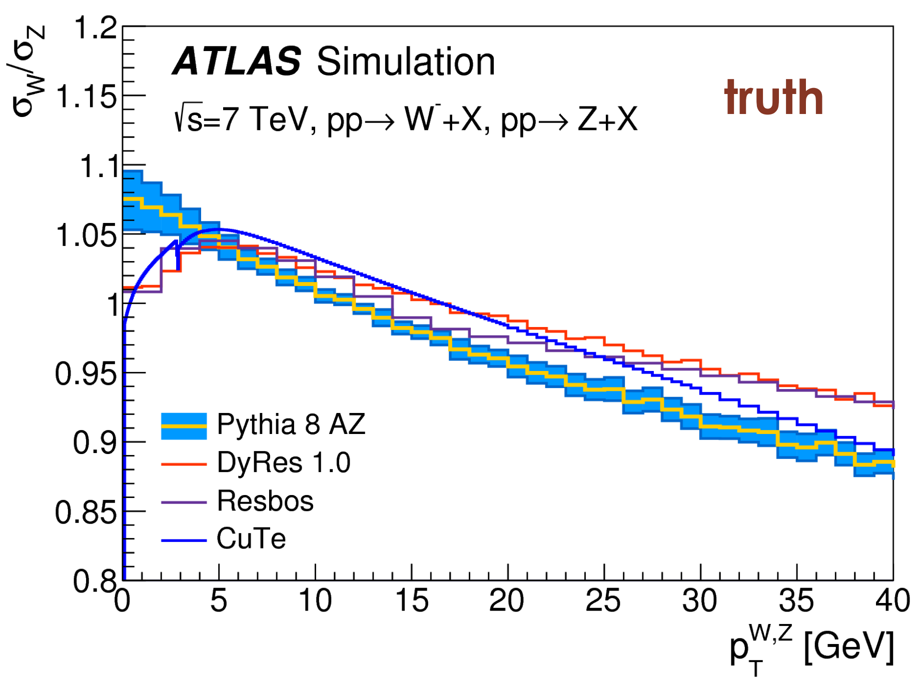

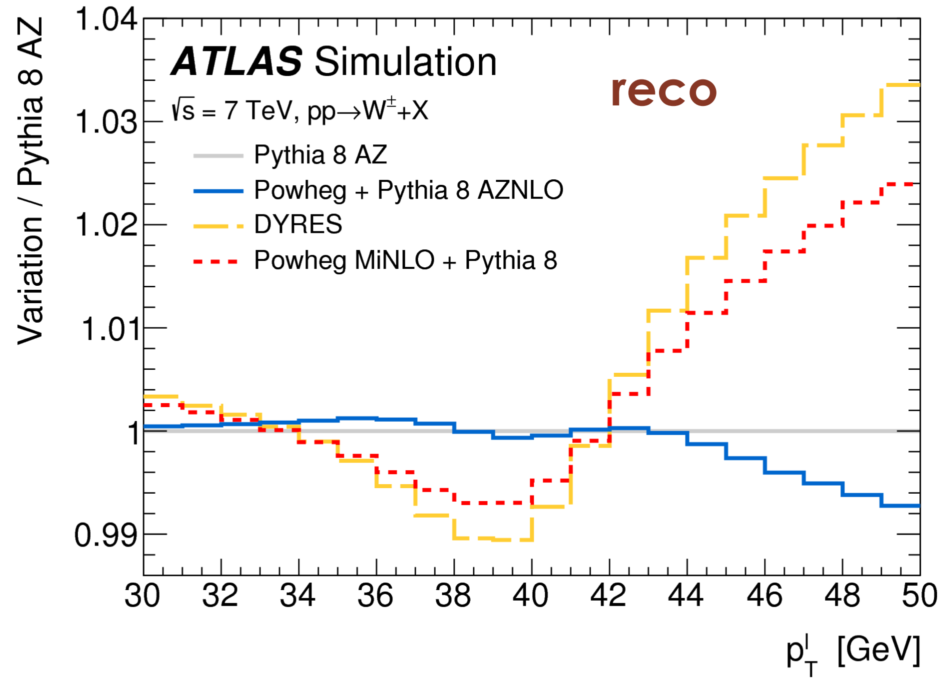

- The effect on m_W of using the "formally" more accurate predictions has a significant impact on the W-mass value of the order of 50-100 MeV

W transverse momentum

- To validate the choice of Pythia8 AZ for the baseline, use u_{ll}^{l} distribution which is very sensitive to the underlying p_T^W distribution
- It provides a data-driven validation of the accuracy of our Pythia8 AZ model and compare to other calculations

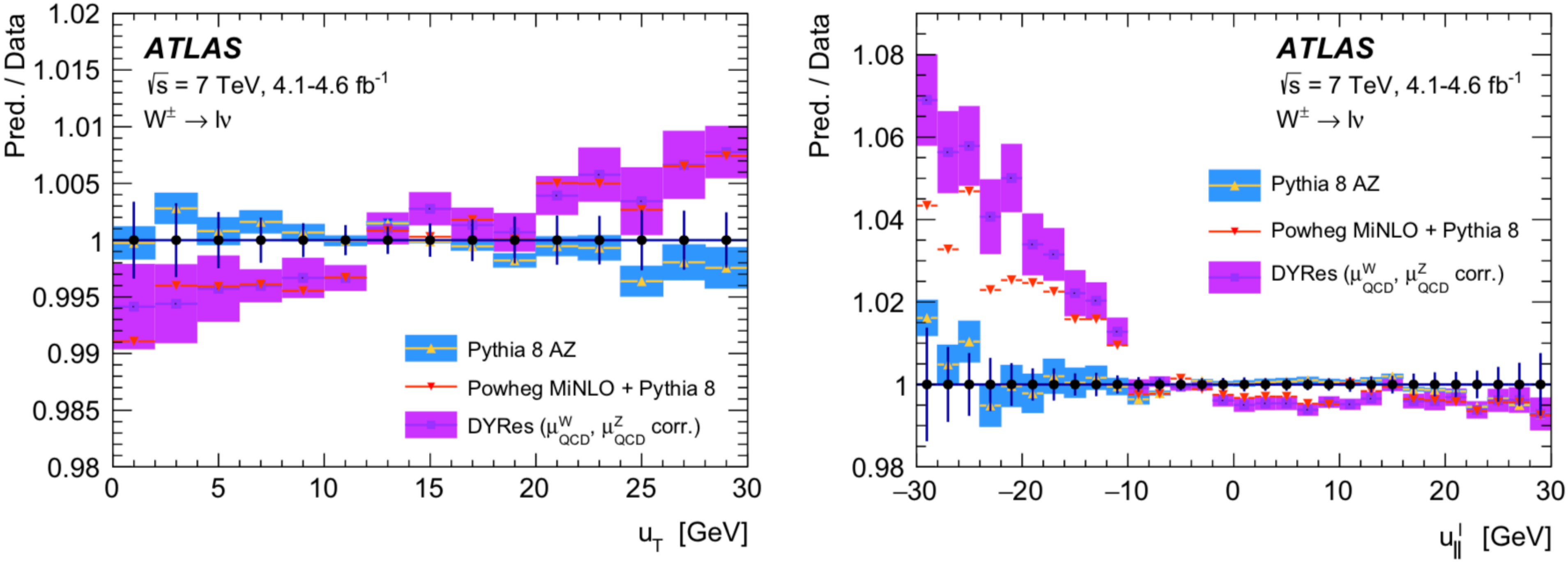

- NLL-resummed predictions and Powheg MiNLO strongly disfavoured by the data, PS MC (Pythia8, Herwig7 and Powheg+Pythia8) in good agreement

p_T^W uncertainties

- Heavy flavour initiated production introduces differences between Z and W and determines a harder p_T spectrum
- Higher order QCD corrections expected to be largely correlated between W and Z produced by light quarks →consider relative variations on p_T^W/p_T^Z under uncertainty variations
- Uncertainty: heavy quark mass variations ($m_c \pm 0.5$ GeV), factorisation scale variations in the QCD ISR (separately for light and heavy-quark induced production)
- Largest deviation of p_T^W/p_T^Z for the PS PDF variation: CTEQ6L1 LO (nominal) to CT14lo, MMHT14lo and NNPDF23lo

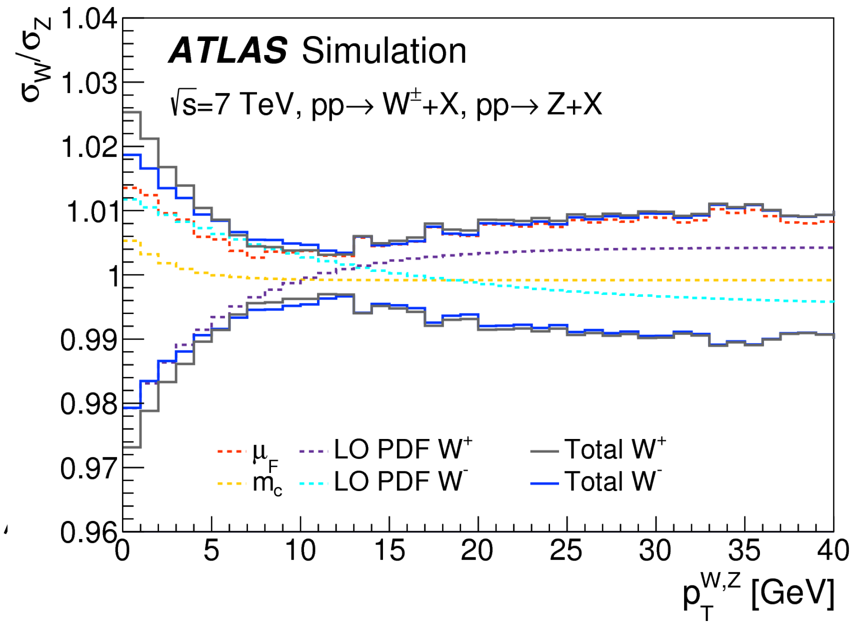

W-boson charge	W^+		W^-		Combined	
Kinematic distribution	p_T^ℓ	m_T	p_T^ℓ	m_T	p_T^ℓ	m_T
Charm-quark mass	1.2	1.5	1.2	1.5	1.2	1.5
Parton shower μ_F with heavy-flavour decorrelation	5.0	6.9	5.0	6.9	5.0	6.9
Parton shower PDF uncertainty	3.6	4.0	2.6	2.4	1.0	1.6

Modelling of the p_T^W

- Ongoing effort in the LHC EW WG to benchmark various different predictions of W/Z p_T ratio
- Aimed at defining a common baseline where all the predictions agree
- Recently q_T-resummation predictions have reached N^{3}LL' accuracy
- However, high-order perturbative accuracy alone is not sufficient for a precise prediction of the W/Z p_T ratio

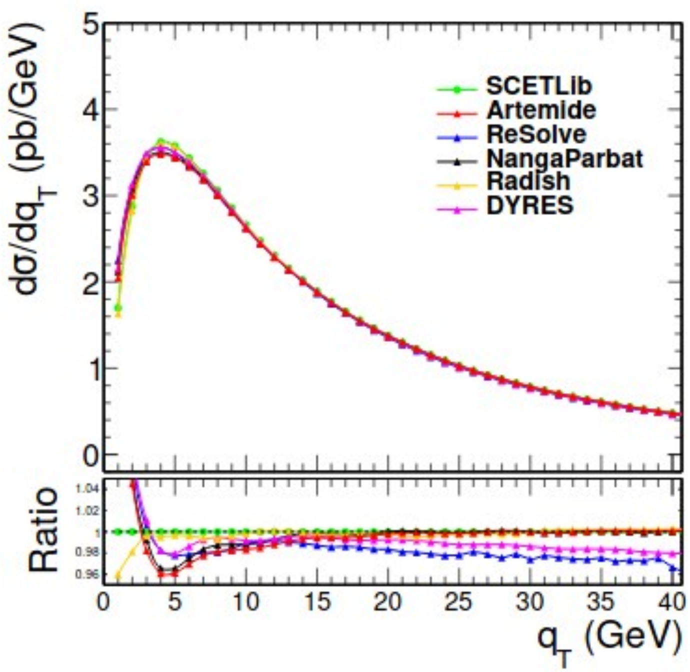

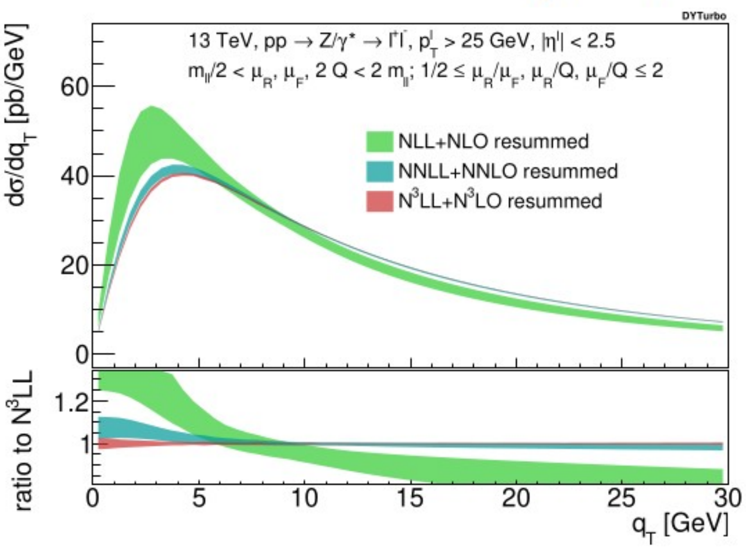

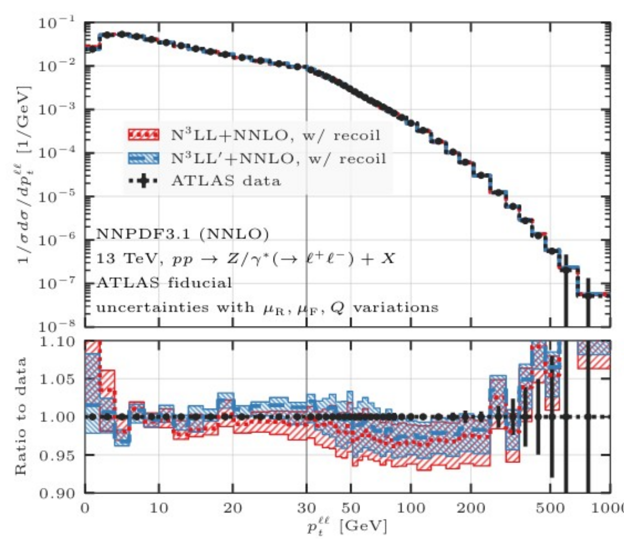

- ***Heavy flavours initiated productions***
- ***Massive quark effects***
- ***Non perturbative QCD***

Fiducial power corrections

- The usage of W asymmetry and Z rapidity measurements to reduce PDF uncertainties for m_W is limited by symmetric fiducial cuts
- Perturbative calculations are affected by enhanced logarithms, connected to the linear dependence of acceptance on the boson p_T e.g. when approaching the limit $p_{T,2} \rightarrow p_{T,1}$ they become unreliable
- The effect is larger when $p_T \sim m_{ll}/2$, at large values of $\cos\theta^*$, as in the CF kinematic region
- Need to resum fiducial power corrections in order to get meaningful predictions
- 2106.08329, 2104.02400, 2006.11382, 2001.02933

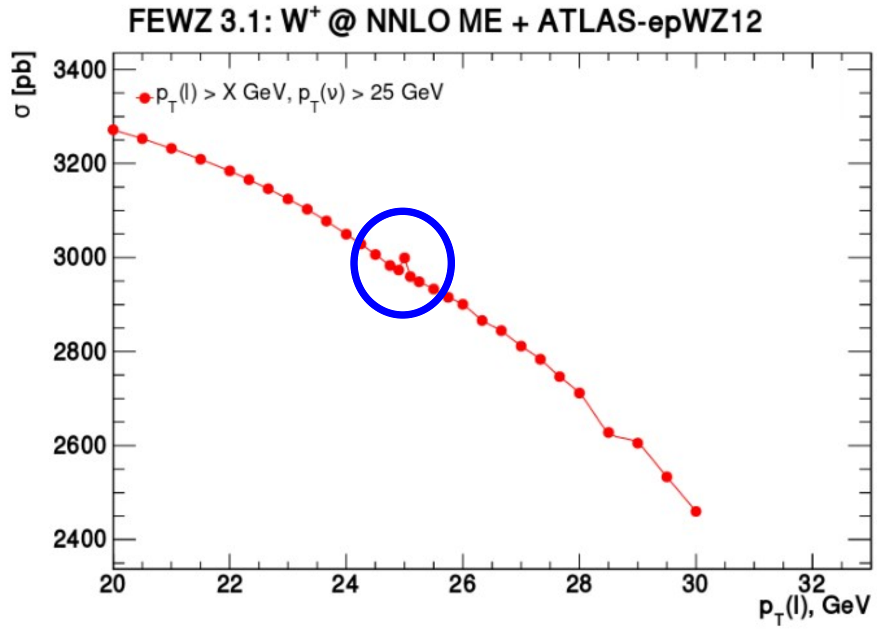

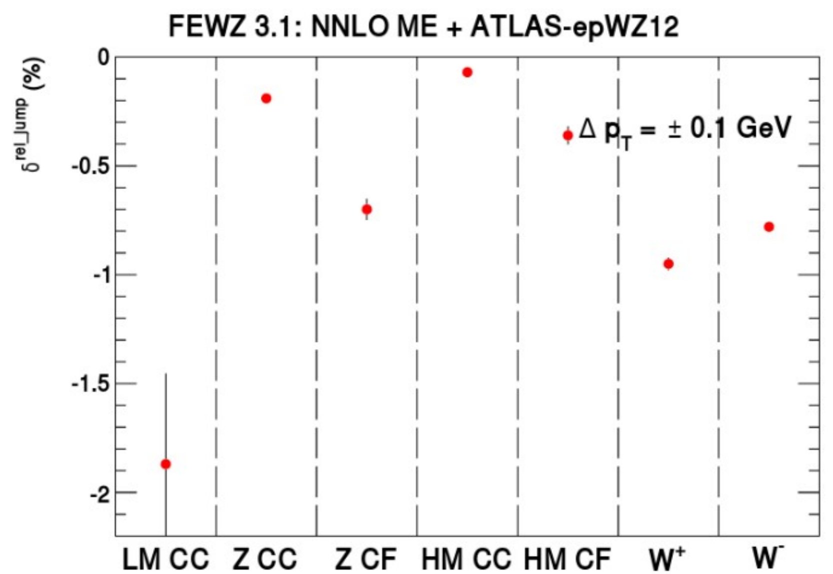

Fiducial power corrections

A. Guida's talk @DIS2022

- Preliminary study, including q_T-resummation in PDF fits to ATLAS W,Z rapidity measurements
- Corrections are significant compared to the experimental accuracy, and gives large improvement in χ^2
- Striking example in the Z CF region, with 10% corrections in the first/last bins

Dataset	CT14 published	CT14 NNLL
ATLAS low mass Z rapidity 2011	11 / 6 →	8.7 / 6
ATLAS peak CC Z rapidity 2011	16 / 12 →	10 / 12
ATLAS peak CF Z rapidity 2011	10 / 9 →	5.6 / 9
ATLAS high mass CC Z rapidity 2011	6.3 / 6	6.3 / 6
ATLAS high mass CF Z rapidity 2011	5.1 / 6	5.4 / 6
ATLAS W- lepton rapidity 2011	8.9 / 11	8.8 / 11
ATLAS W+ lepton rapidity 2011	10 / 11	10 / 11
Correlated χ^2	39 →	35
Log penalty χ^2	-4.11	-3.60
Total χ^2 / dof	103 / 61 →	86 / 61
χ^2 p-value	0.00	0.02

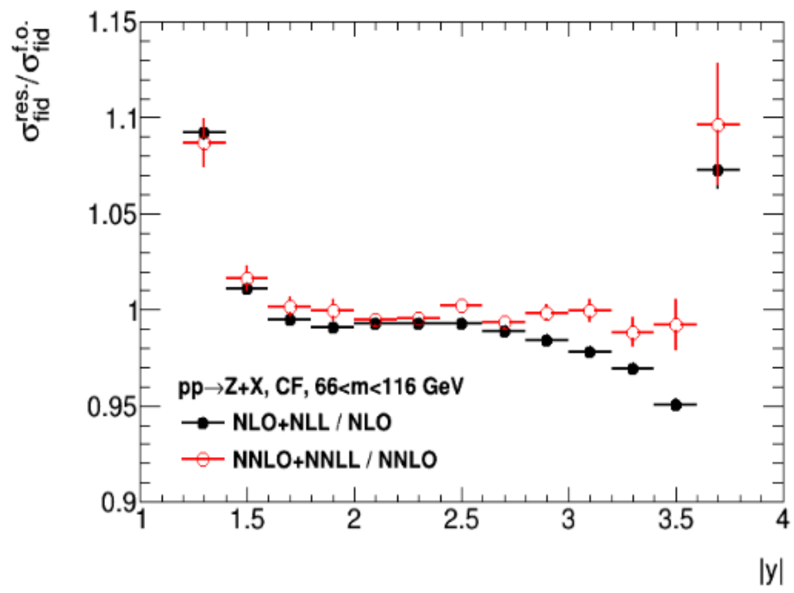

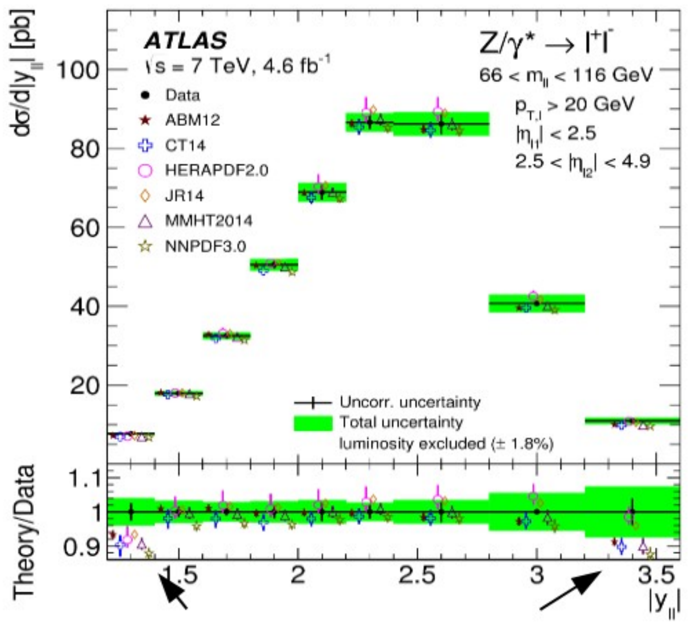

Control kinematic distributions

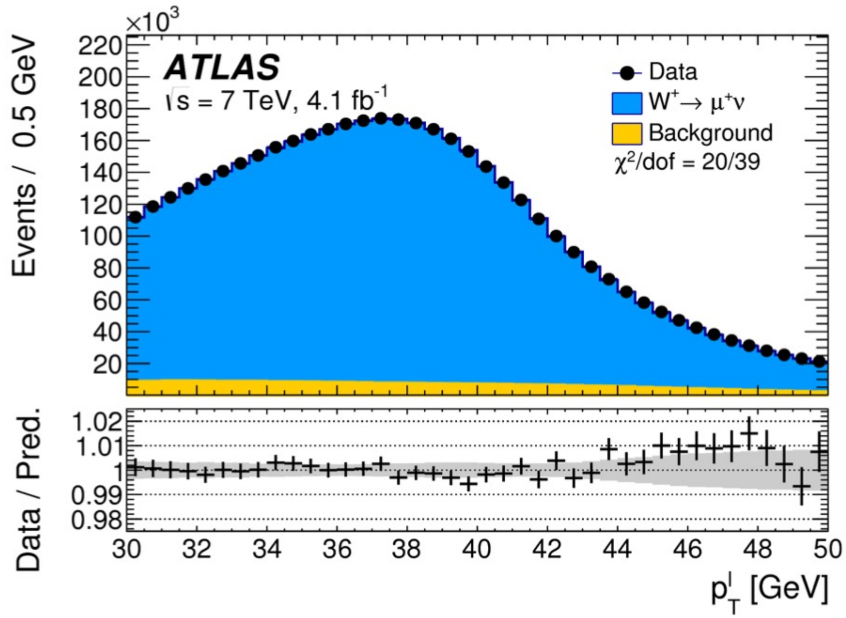

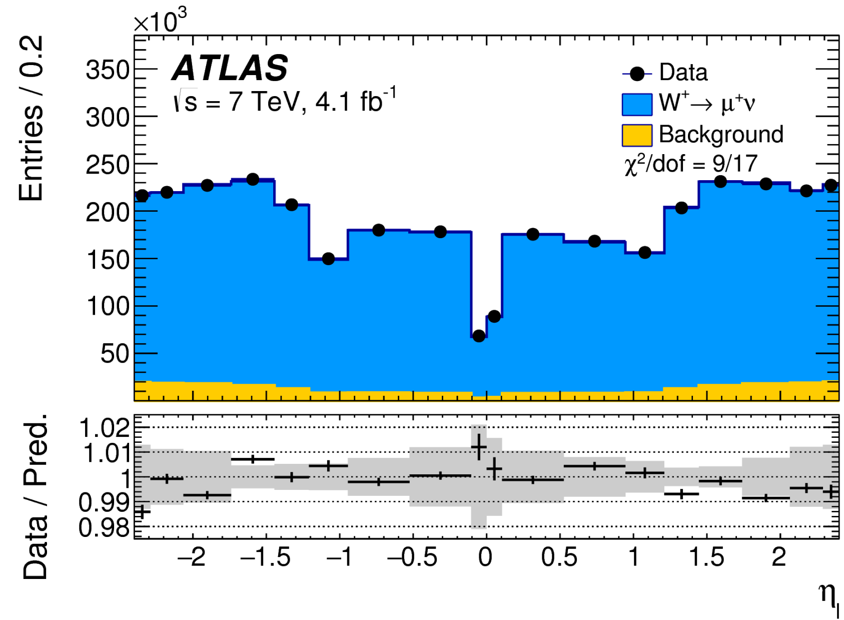

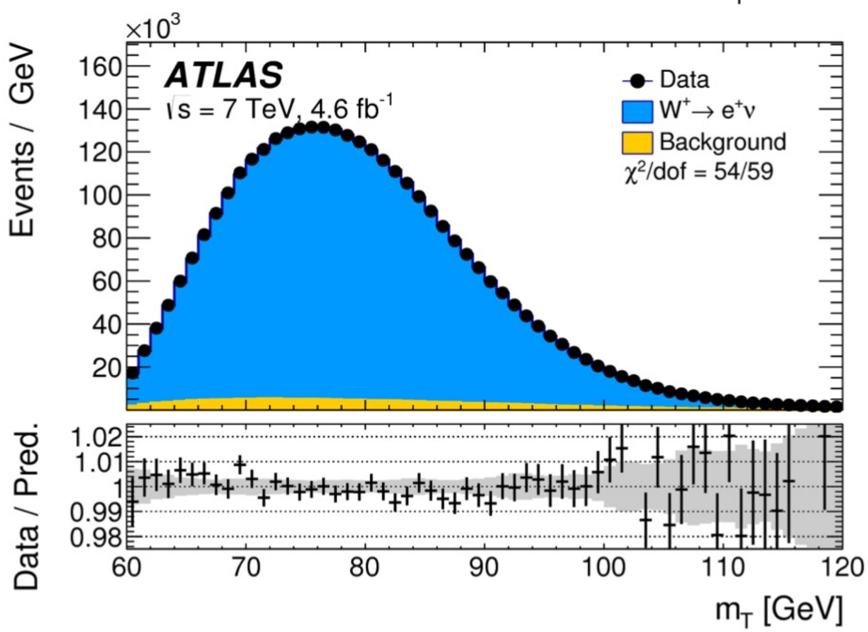

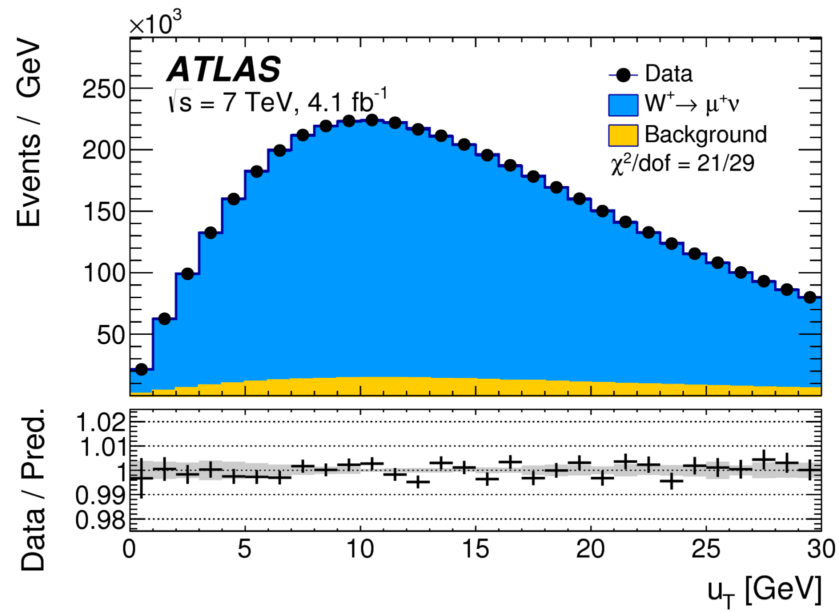

Control kinematic distributions

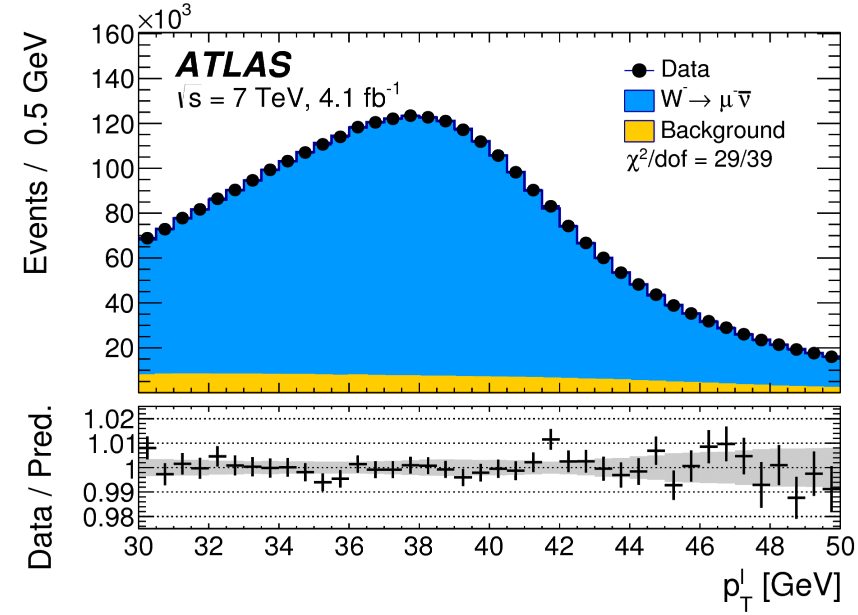

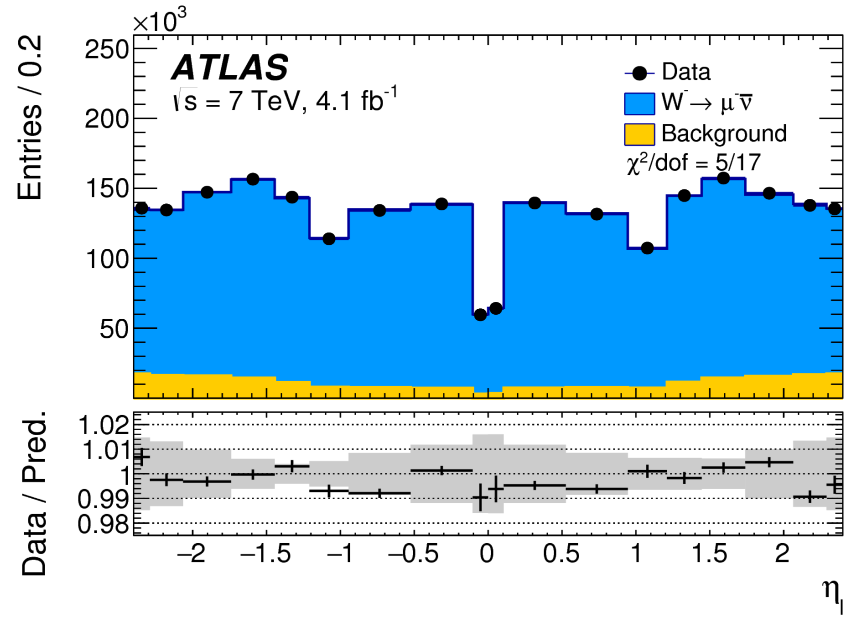

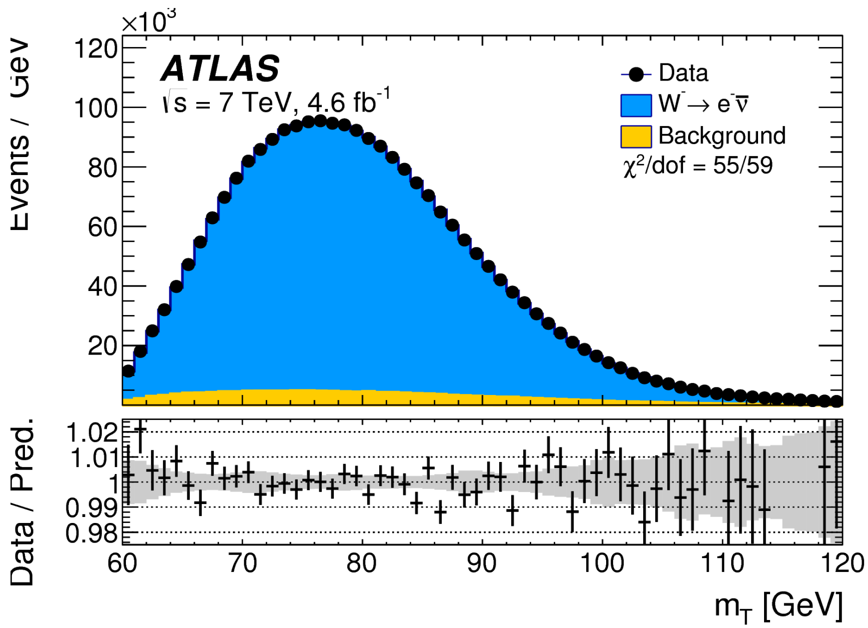

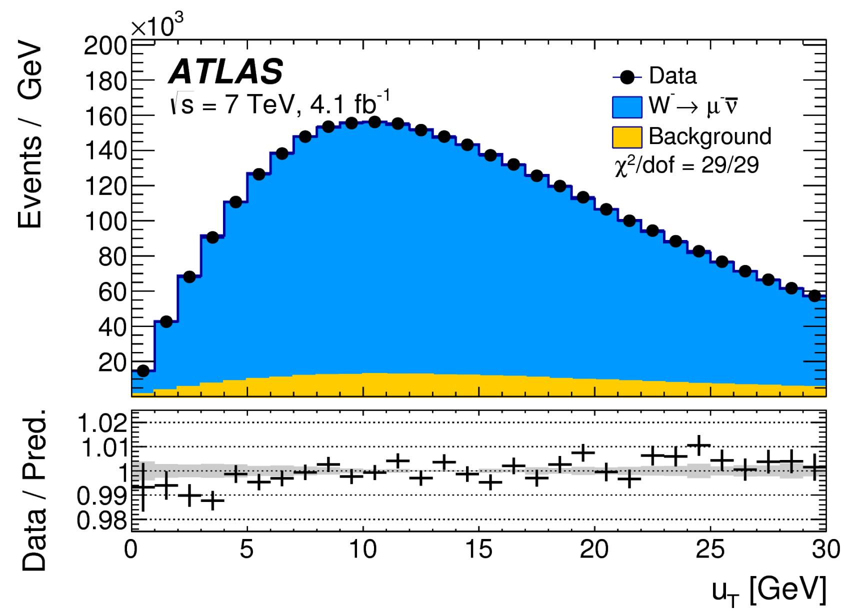

Measurement strategy - categories

- A crucial aspect of the measurement design is the categorisation
  - Events are categorised according to their type and kinematic range
  - Validate detector calibration and physics modelling and improve accuracy
- The various set of categories are sensitive to different experimental and theoretical biased → the consistency of m_W across categories validate our knowledge of the detector and of QCD
- The experimental and theoretical uncertainties have different correlation or anticorrelation patterns
  - The categorisation allows to constrain them and increase the sensitivity to m_W
- Categories used for the combination (28 in total):

Decay channel	$W \to e\nu$	$W \to \mu\nu$
Kinematic distributions	p_{T}^{ℓ}, m_{T}	p_{T}^{ℓ}, m_{T}
Charge categories	W^+, W^-	W^+, W^-
$\lvert\eta_\ell\rvert$ categories	$[0, 0.6]$, $[0.6, 1.2]$, $[1.8, 2.4]$	$[0, 0.8]$, $[0.8, 1.4]$, $[1.4, 2.0]$, $[2.0, 2.4]$

Measurement categories

Channel	m_W [MeV]	Stat. Unc.	Muon Unc.	Elec. Unc.	Recoil Unc.	Bckg. Unc.	QCD Unc.	EW Unc.	PDF Unc.	Total Unc.
m_T-Fit										
$W^+ \to \mu\nu, \lvert\eta\rvert < 0.8$	80371.3	29.2	12.4	0.0	15.2	8.1	9.9	3.4	28.4	47.1
$W^+ \to \mu\nu, 0.8 < \lvert\eta\rvert < 1.4$	80354.1	32.1	19.3	0.0	13.0	6.8	9.6	3.4	23.3	47.6
$W^+ \to \mu\nu, 1.4 < \lvert\eta\rvert < 2.0$	80426.3	30.2	35.1	0.0	14.3	7.2	9.3	3.4	27.2	56.9
$W^+ \to \mu\nu, 2.0 < \lvert\eta\rvert < 2.4$	80334.6	40.9	112.4	0.0	14.4	9.0	8.4	3.4	32.8	125.5
$W^- \to \mu\nu, \lvert\eta\rvert < 0.8$	80375.5	30.6	11.6	0.0	13.1	8.5	9.5	3.4	30.6	48.5
$W^- \to \mu\nu, 0.8 < \lvert\eta\rvert < 1.4$	80417.5	36.4	18.5	0.0	12.2	7.7	9.7	3.4	22.2	49.7
$W^- \to \mu\nu, 1.4 < \lvert\eta\rvert < 2.0$	80379.4	35.6	33.9	0.0	10.5	8.1	9.7	3.4	23.1	56.9
$W^- \to \mu\nu, 2.0 < \lvert\eta\rvert < 2.4$	80334.2	52.4	123.7	0.0	11.6	10.2	9.9	3.4	34.1	139.9
$W^+ \to e\nu, \lvert\eta\rvert < 0.6$	80352.9	29.4	0.0	19.5	13.1	15.3	9.9	3.4	28.5	50.8
$W^+ \to e\nu, 0.6 < \lvert\eta\rvert < 1.2$	80381.5	30.4	0.0	21.4	15.1	13.2	9.6	3.4	23.5	49.4
$W^+ \to e\nu, 1,8 < \lvert\eta\rvert < 2.4$	80352.4	32.4	0.0	26.6	16.4	32.8	8.4	3.4	27.3	62.6
$W^- \to e\nu, \lvert\eta\rvert < 0.6$	80415.8	31.3	0.0	16.4	11.8	15.5	9.5	3.4	31.3	52.1
$W^- \to e\nu, 0.6 < \lvert\eta\rvert < 1.2$	80297.5	33.0	0.0	18.7	11.2	12.8	9.7	3.4	23.9	49.0
$W^- \to e\nu, 1.8 < \lvert\eta\rvert < 2.4$	80423.8	42.8	0.0	33.2	12.8	35.1	9.9	3.4	28.1	72.3
p_T-Fit										
$W^+ \to \mu\nu, \lvert\eta\rvert < 0.8$	80327.7	22.1	12.2	0.0	2.6	5.1	9.0	6.0	24.7	37.3
$W^+ \to \mu\nu, 0.8 < \lvert\eta\rvert < 1.4$	80357.3	25.1	19.1	0.0	2.5	4.7	8.9	6.0	20.6	39.5
$W^+ \to \mu\nu, 1.4 < \lvert\eta\rvert < 2.0$	80446.9	23.9	33.1	0.0	2.5	4.9	8.2	6.0	25.2	49.3
$W^+ \to \mu\nu, 2.0 < \lvert\eta\rvert < 2.4$	80334.1	34.5	110.1	0.0	2.5	6.4	6.7	6.0	31.8	120.2
$W^- \to \mu\nu, \lvert\eta\rvert < 0.8$	80427.8	23.3	11.6	0.0	2.6	5.8	8.1	6.0	26.4	39.0
$W^- \to \mu\nu, 0.8 < \lvert\eta\rvert < 1.4$	80395.6	27.9	18.3	0.0	2.5	5.6	8.0	6.0	19.8	40.5
$W^- \to \mu\nu, 1.4 < \lvert\eta\rvert < 2.0$	80380.6	28.1	35.2	0.0	2.6	5.6	8.0	6.0	20.6	50.9
$W^- \to \mu\nu, 2.0 < \lvert\eta\rvert < 2.4$	80315.2	45.5	116.1	0.0	2.6	7.6	8.3	6.0	32.7	129.6
$W^+ \to e\nu, \lvert\eta\rvert < 0.6$	80336.5	22.2	0.0	20.1	2.5	6.4	9.0	5.3	24.5	40.7
$W^+ \to e\nu, 0.6 < \lvert\eta\rvert < 1.2$	80345.8	22.8	0.0	21.4	2.6	6.7	8.9	5.3	20.5	39.4
$W^+ \to e\nu, 1,8 < \lvert\eta\rvert < 2.4$	80344.7	24.0	0.0	30.8	2.6	11.9	6.7	5.3	24.1	48.2
$W^- \to e\nu, \lvert\eta\rvert < 0.6$	80351.0	23.1	0.0	19.8	2.6	7.2	8.1	5.3	26.6	42.2
$W^- \to e\nu, 0.6 < \lvert\eta\rvert < 1.2$	80309.8	24.9	0.0	19.7	2.7	7.3	8.0	5.3	20.9	39.9
$W^- \to e\nu, 1.8 < \lvert\eta\rvert < 2.4$	80413.4	30.1	0.0	30.7	2.7	11.5	8.3	5.3	22.7	51.0

Summary of corrections

- After all the corrections are applied, consistent results are achieved between different channels, observables, categories, charges
- Only after, results were unblinded

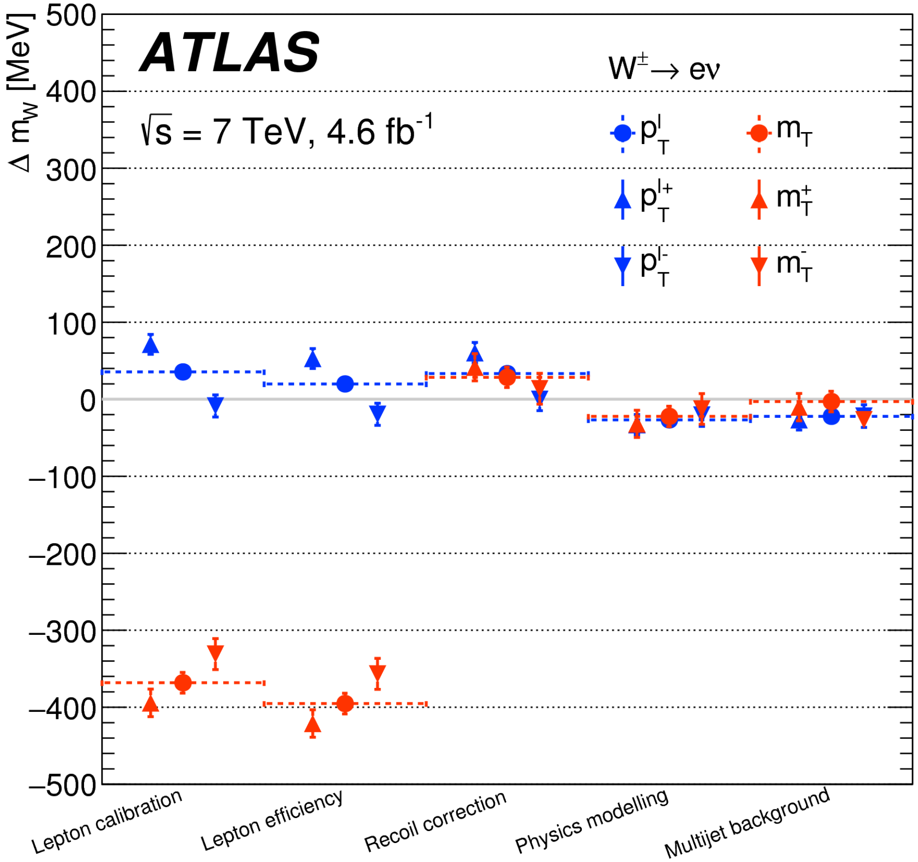

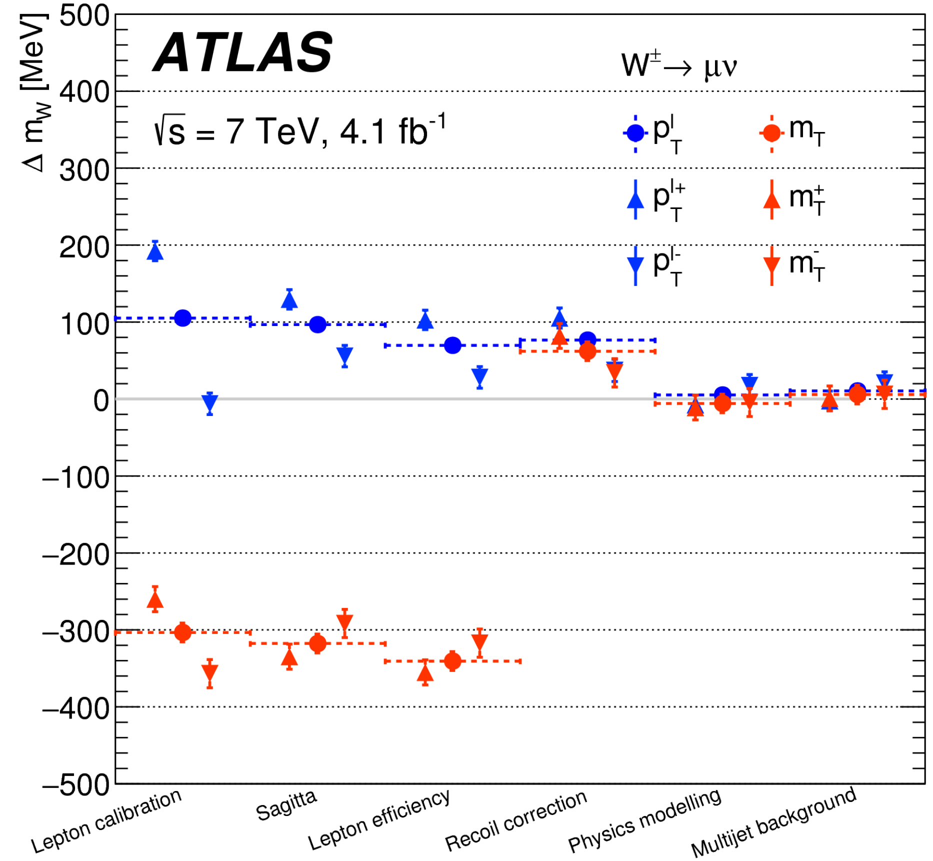

Prospects and challenges

ATLAS W mass at 7 TeV

Combination	Weight
Electrons	0.427
Muons	0.573
m_{T}	0.144
p_{T}^{ℓ}	0.856
W^{+}	0.519
W^{-}	0.481

- The lepton p_T distribution dominates over m_T already with 7 teV data
- Muon channel more important than electron channel

- Two possible paths for future measurements:
  - Standard high pileup data, measurement dominated by lepton p_T → Challenges: W/Z p_T modelling, lepton p_T calibration
  - Low pileup data, measurement dominated by m_T → Challenges: recoil calibration
- Orthogonal approaches, with different dominant uncertainties
- Should be both pursued, will benefit from the combination

Prospects for m_W at the HL-LHC

- Increased acceptance provided by the new inner detector in ATLAS (ITK) extends the coverage up to $|\eta| < 4$
- This allows futher constraints on PDFs from cross section measurements
- With 1 fb^{-1} of low pileup data ($<\mu> \sim \mathbf{2}$) likely to reach ~6 MeV of stat+PDF uncertainty
- LHeC/EIC ep collisions would largely reduce PDF uncertainties (< 2 MeV)

ATLAS-PUB-2018-026

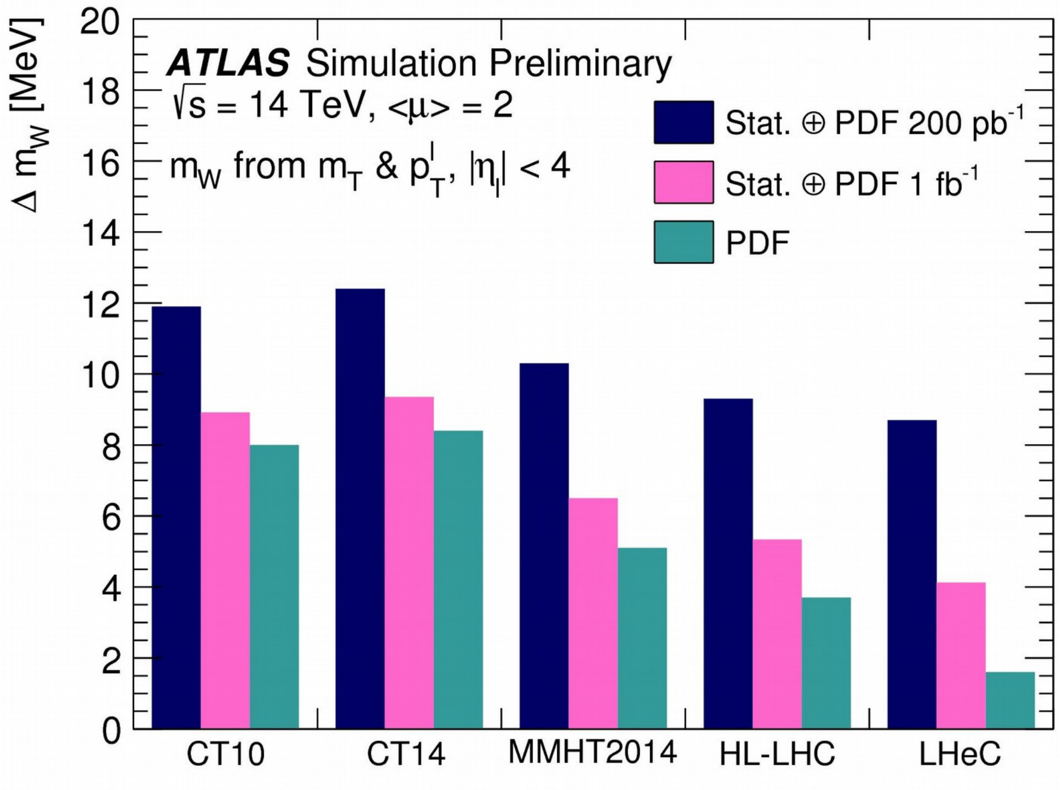

m_W at the LHC with high pileup data

- The statistical uncertainty is expected to be reduced by factors of 2 to 7 by analysing 8 and 13 TeV data sets

$\sqrt{s}$	7 TeV	8 TeV	13 TeV
Luminosity	~4.5 fb^{-1}	~20 fb^{-1}	~140 fb^{-1}
Events	1.5·10^{7}	8.0·10^{7}	8.4·10^{8}
Stat. Unc. [MeV]	7	3	1

- PDF uncertainties will be reduced by the inclsuion of the latest HERA and W asymmetry data in the global PDF fits (expected a ~30% reduction)

- EW uncertainties can be largely reduced by including available HO corrections

- p_T^W can be reduced by using analytic resummation at NNLL (if calculations improve agreement with the data)

- Muon calibration can be improved using J/ψ data

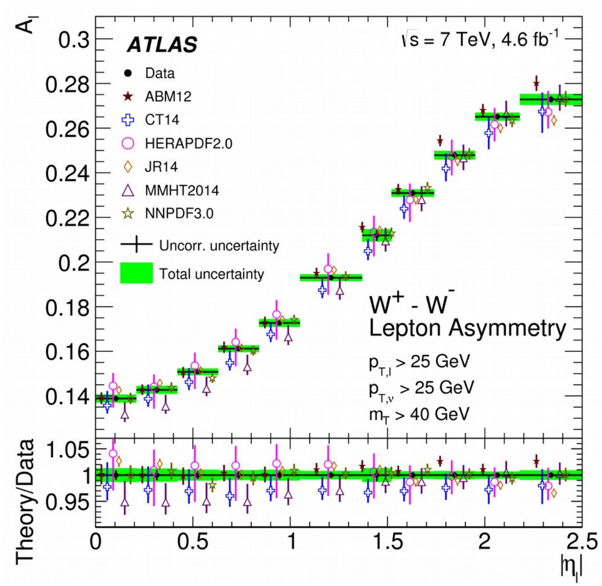

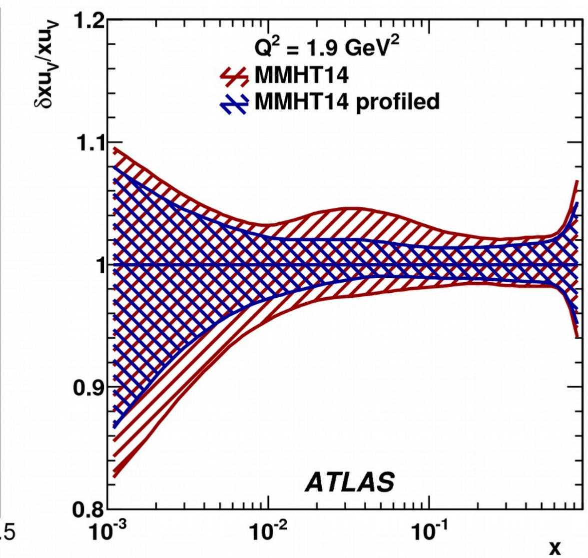

m_W at future colliders

- The ultimate precision on m_W can be achieved at e^+e^- colliders trough an energy scan of the WW production threshold

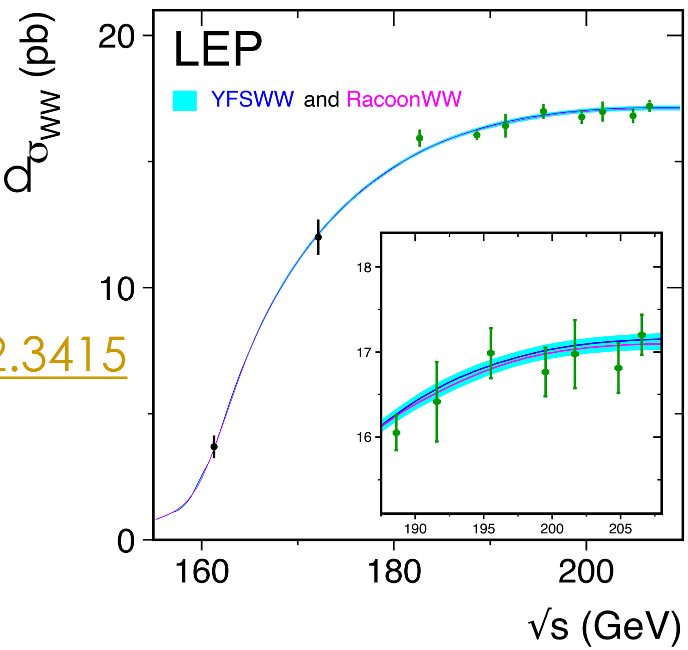

1302.3415

- Near threshold, the WW cross section is proportional to the non-relativistic W velocity

1306.6352 $\sigma(WW) \propto \beta_W$

- ILC Giga-Z program:
  - Energy scan 160 – 170 GeV
  - δm_W = 6-7 MeV
- FCC-ee WW program:
  - δm_W = 0.5 MeV
  - Dominated by statistical uncertainties
- Dominant uncertainties:
  - Initial state QED corrections
  - Parametrisation of cross section near threshold

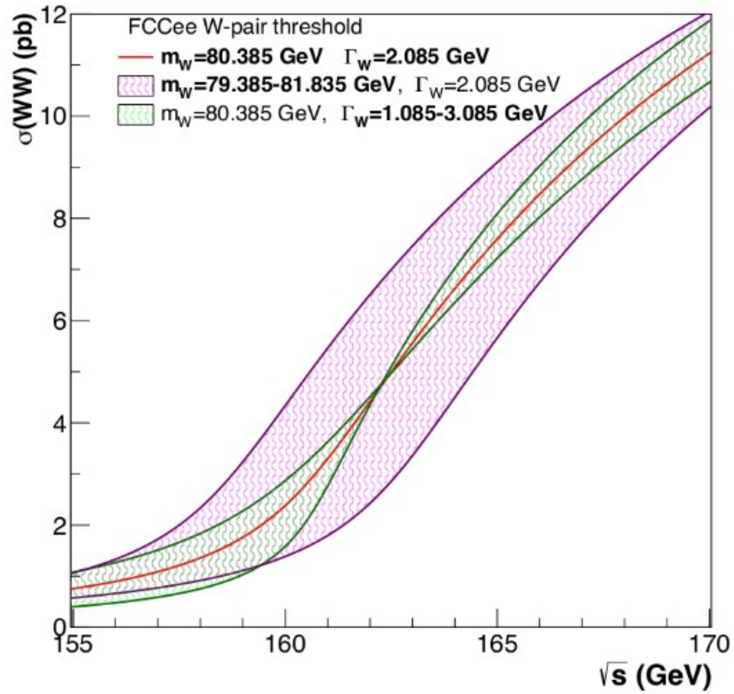

Reducing PDF uncertainties

- Drell-Yan data provide high sensitivity to PDFs
- They feature small systematics (both theoretical and experimental), high statistical precision and good control of correlations
- Recent studies have established the remarkable potential of less traditional observables such as:
  - the forward-backward asymmetry (A_{FB}) - JHEP 10 (2019) 176
  - the A_0 angular coefficient - Phys. Lett. B 821 (2021) 136613
- The potential of the lepton-charge asymmetry (A_W) in constraining PDFs has been also investigated - Nuclear Physics B 968 (2021) 115444
- The impact of improving the PDF systematic on the experimental sensitivity of W' and Z' searches at the LHC has been studied - JHEP 02 (2022) 179
- Benchmark model: 4-Dimensional Composite Higgs Model (4DCHM) realization of the the minimal composite Higgs model – JHEP 04 (2012) 042, Nucl. Phys. B 719 (2005) 165
- Two parameters of interest: the compositeness scale f and the coupling of the new resonance g_ρ

Drell-Yan asymmetry measurements

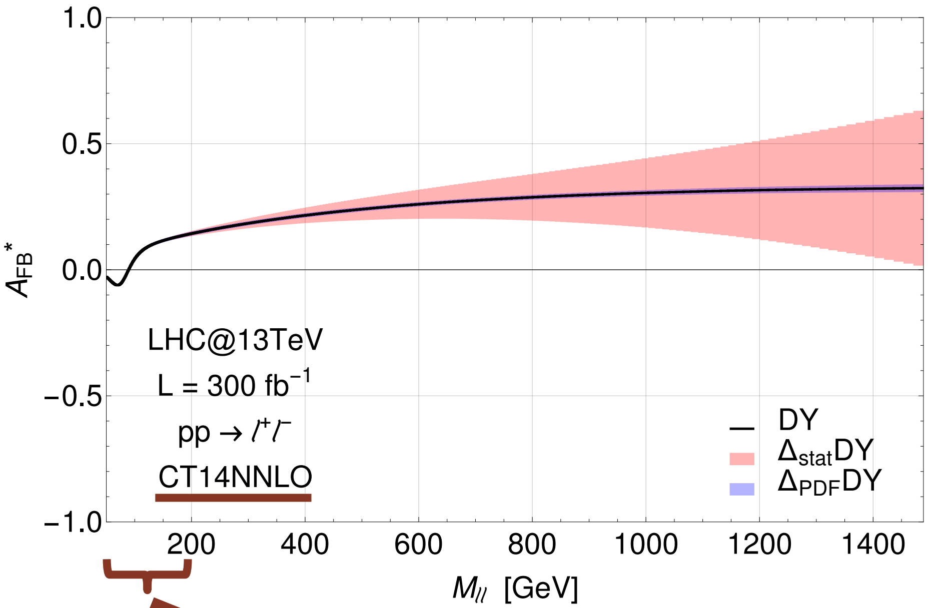

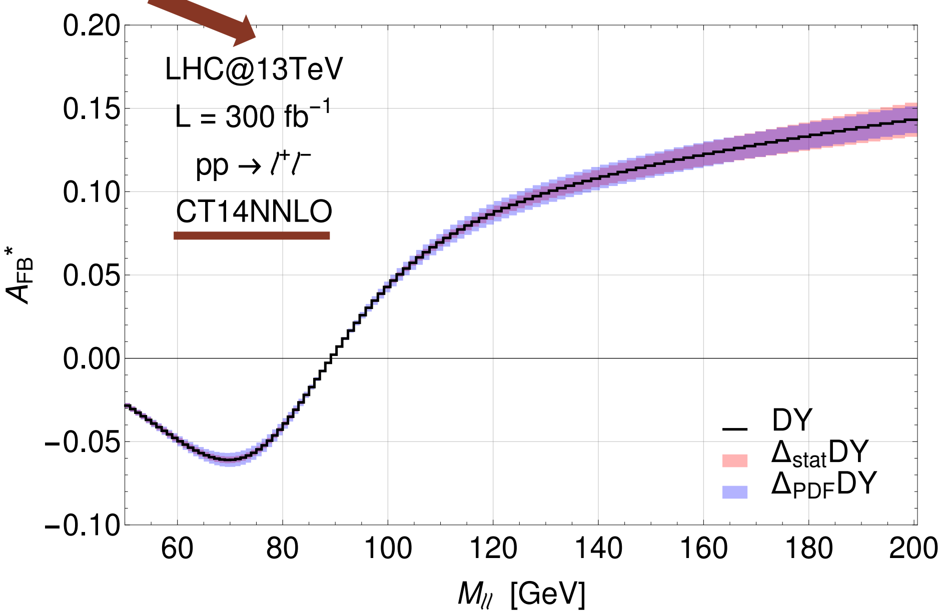

- At LO, angle defined w.r.t. the direction of the boost of the di-lepton system
- At NLO, angle defined in the Collin-Soper frame: $\cos\theta^* = \frac{p_{Z,ll}}{M_{ll}|p_{Z,ll}|} \frac{p_1^+ p_2^- - p_1^- p_2^+}{\sqrt{M_{ll}^2 + p_{T,ll}^2}}$

  where $p_i^\pm = E_i \pm p_{Z,i}$
- $\sigma_F = \int_0^1 \frac{d\sigma}{d\cos\theta^*} d\cos\theta^*$
- $\sigma_B = \int_{-1}^0 \frac{d\sigma}{d\cos\theta^*} d\cos\theta^*$

$$A_{FB} = \frac{\sigma_F - \sigma_B}{\sigma_F + \sigma_B}$$

- A_{FB} has smaller systematic but larger statistical error compared to cross section measurements
- Sensitive to ($2/3u_V + 1/3d_V$) and complementary to DY Charged Current asymmetry (u_V - d_V)
- High-invariant mass region: dominated by statistical uncertainties
- $m_{l^+l^-} \simeq m_Z$: high-stats to perform very precise measurements

Setup of the xFitter analysis

- Datafiles with pseudo-data generated for several PDF sets within xFitter
- **NLO AFB central values:** 62 bins of 2.5 GeV-width from 45 to 200 GeV
- NNLO QCD mass dependent k-factor included for estimating the number of events in each invariant mass bin R. V. Harlander and W. B. Kilgore, Phys. Rev. Lett. 88, 201801 (2002)
- No sensible difference LO analytic and LO from APPLgrid
- Various lower rapidity cuts applied:
  - |Y| > 0 (no cut applied)
  - |Y| > 1.5
  - |Y| > 4.0 (only at LO)
- Profiling exercise on 5 different PDF sets:
  - ABMP16NNLO
  - CT14nnlo
  - HERAPDF2.0nnlo (EIG)
  - MMHT14nnlo
  - NNPDF3.1nnlo (Hessian set)

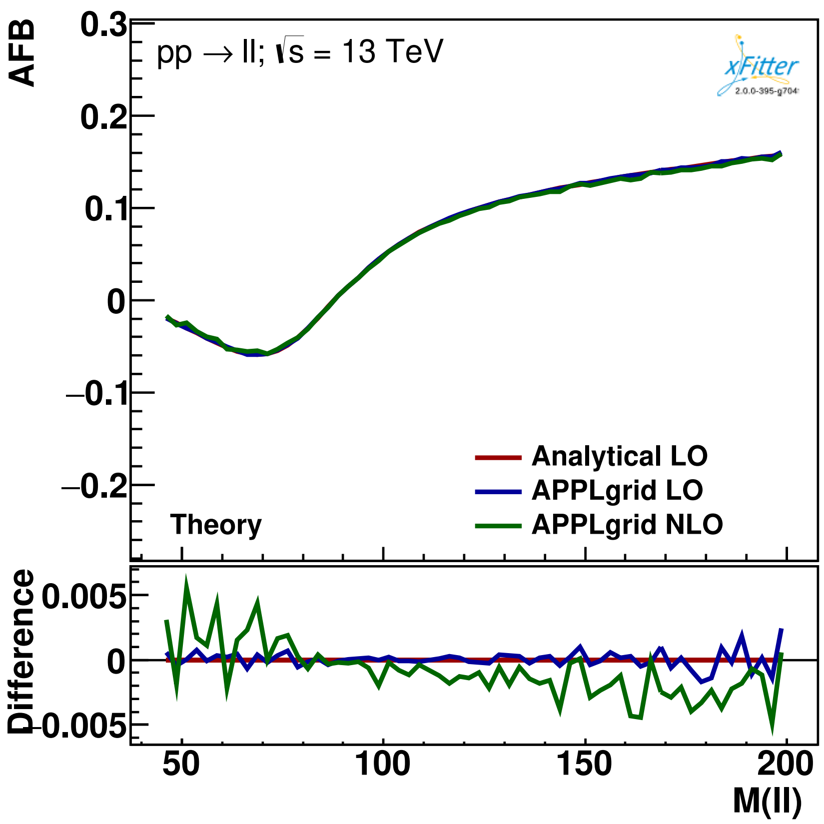

The lepton-charged asymmetry

- Defined as:

$$A_W = \frac{d\sigma/d|\eta_\ell|(W^+ \to \ell^+\nu) - d\sigma/d|\eta_\ell|(W^- \to \ell^-\bar{\nu})}{d\sigma/d|\eta_\ell|(W^+ \to \ell^+\nu) + d\sigma/d|\eta_\ell|(W^- \to \ell^-\bar{\nu})}$$

- NLO QCD predictions from APPLgrid
- NNLO QCD + NLO EW accuracy achieved using k_F
- Data well described by modern PDFs

PDF set	χ^2/d.o.f.
CT18NNLO	10.26/11
CT18ANNLO	11.29/11
MSHT20nnlo_as118	12.18/11
NNPDF3.1_nnlo_as_0118_hessian	14.88/11
PDF4LHC15_nnlo_100	9.53/11
ABMP16_5_nnlo	18.21/11
HERAPDF20_NNLO_EIG	8.92/11

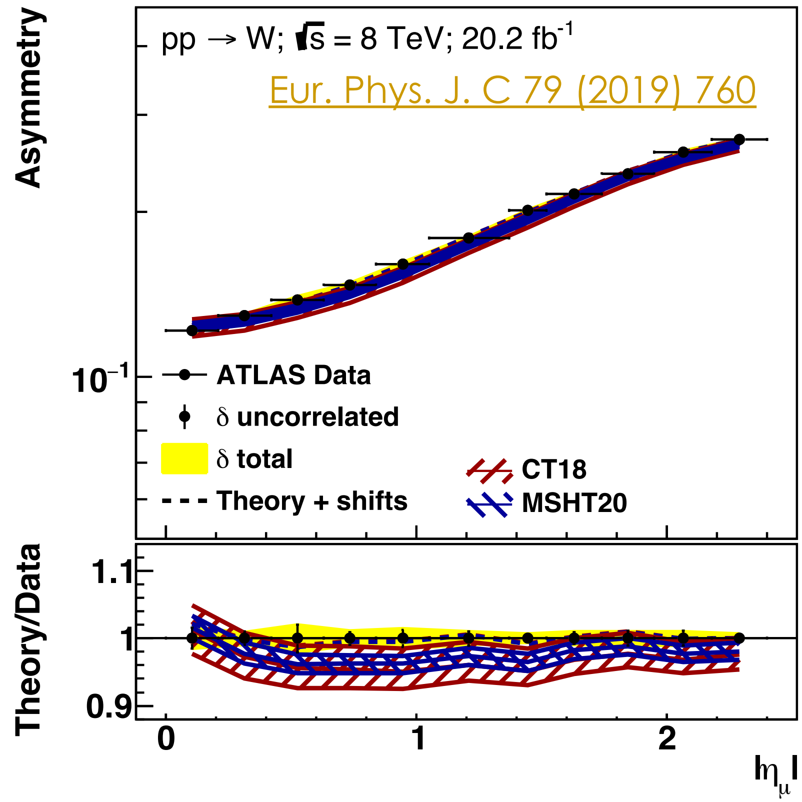

- A_W pseudodata at $\sqrt{s}$ = 13 TeV for different luminosities:
  - 300 fb^{-1} (end of LHC Run III)
  - 3 ab^{-1} (HL-LHC stage)

A_W VS A_{FB}

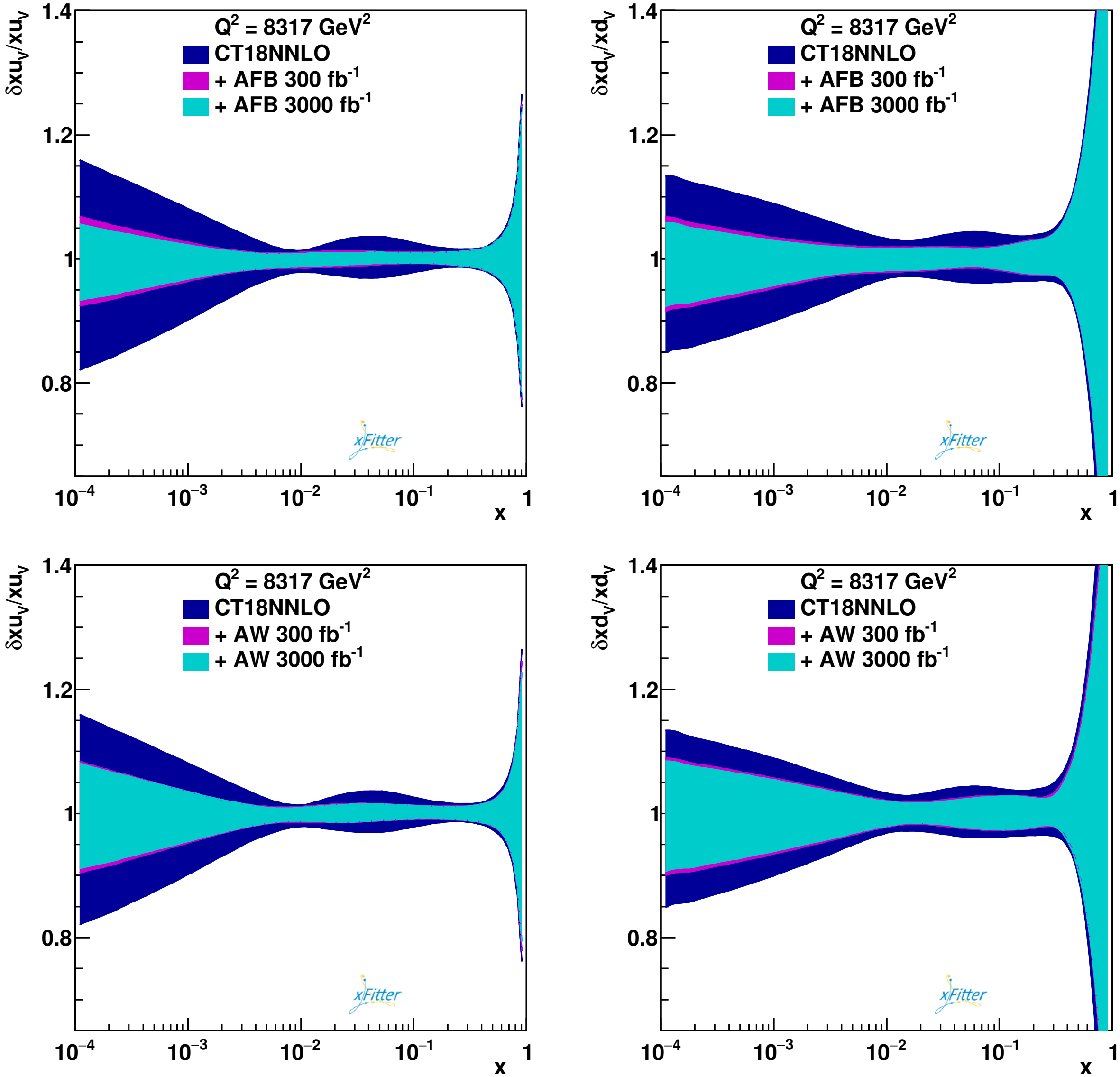

- Comparable sensitivity on valence quark PDFs
- A_W largely sensitivity to $x(d_V - u_V)$
- Complementary wrt A_{FB} - mostly sensitive to $x(1/3\ d_V + 2/3\ u_V)$
- Strong reduction of PDF uncertainties at low-x
- A_{FB} provides slightly stronger constraints
- Saturation of uncertainty reduction from 300 fb^{-1} to 3 ab^{-1}

Combining A_W and A_{FB}

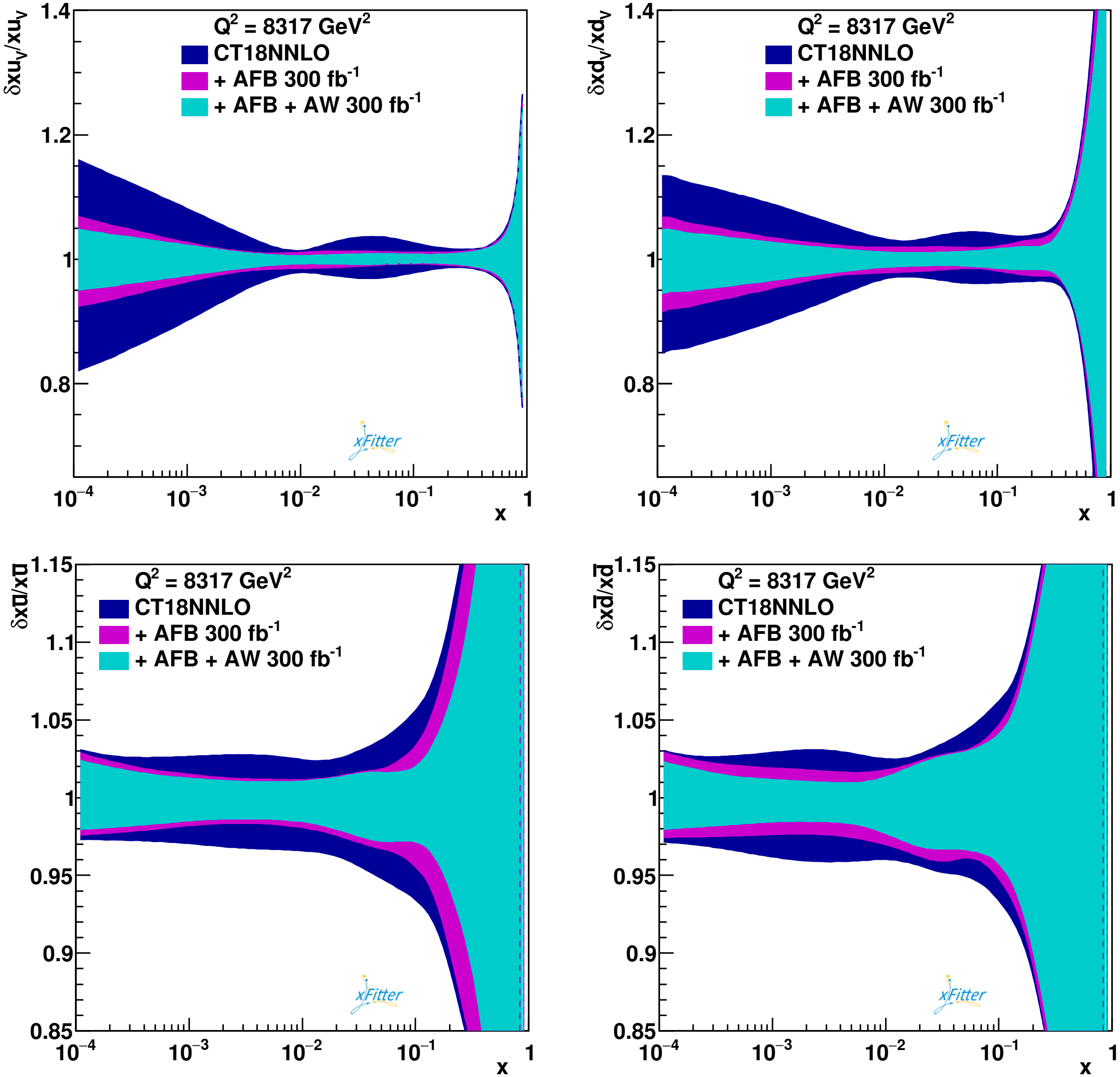

- The combination of A_W and A_{FB} can further reduce the PDF bands
- Strong reduction of PDF uncertainties at low- and intermediate-x
- $x\bar{u}$ and $x\bar{d}$ show reduced bands at high-x as well

Implications on BSM searches

- We studied the reduction of uncertainties in the high invariant mass spectra for BSM searches

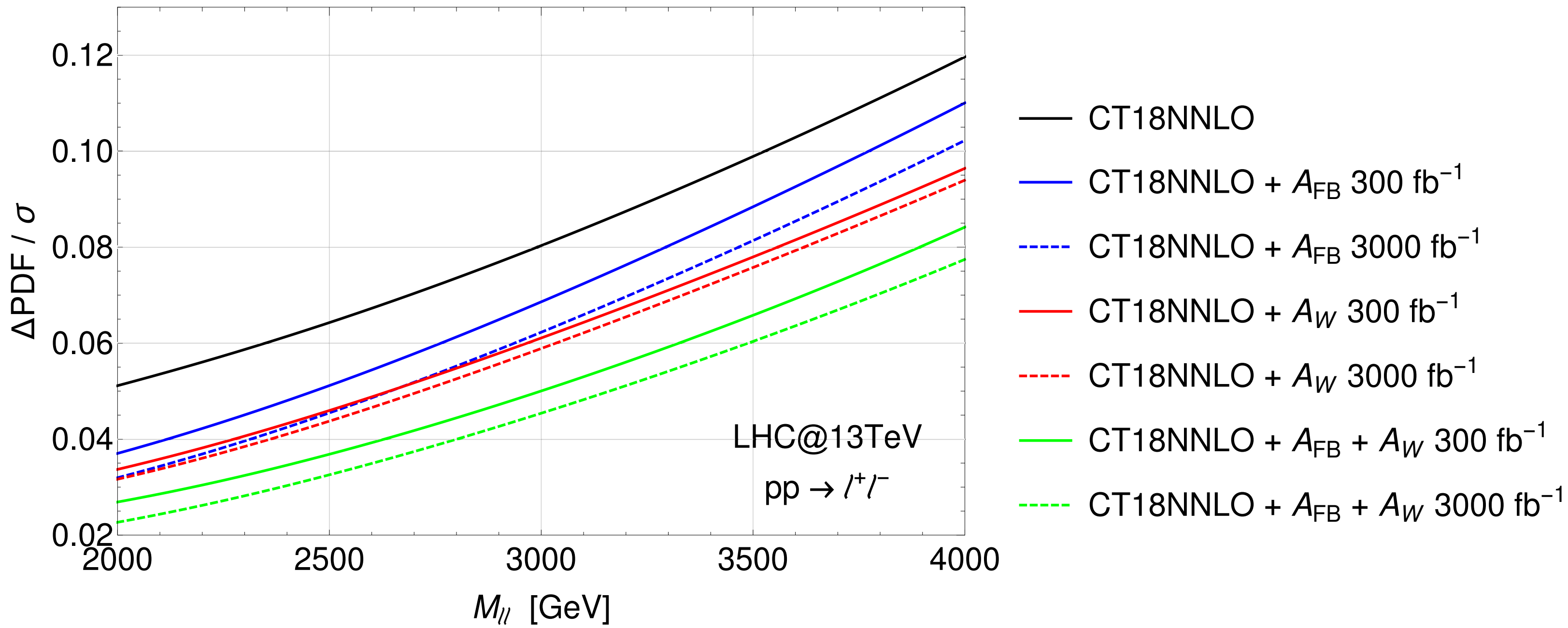

- Original PDF uncertainty (i.e.) at 4 TeV from 11.9% is reduced to:
  - 11% (10.2%) by A_{FB} 300 (3000) fb^{-1} data
  - 9.6% (9.4%) by A_W 300 (3000) fb^{-1} data
  - 8.4% (7.8%) by combination of A_{FB} and A_W 300 (3000) fb^{-1} data

Implications on BSM searches

- PDF uncertainties are relevant in searches for non-resonant objects
- Enhanced SSM model ($g_{eSSM} = 3g_{SSM}$) – Phys. Lett. B 803 (2020) 135293

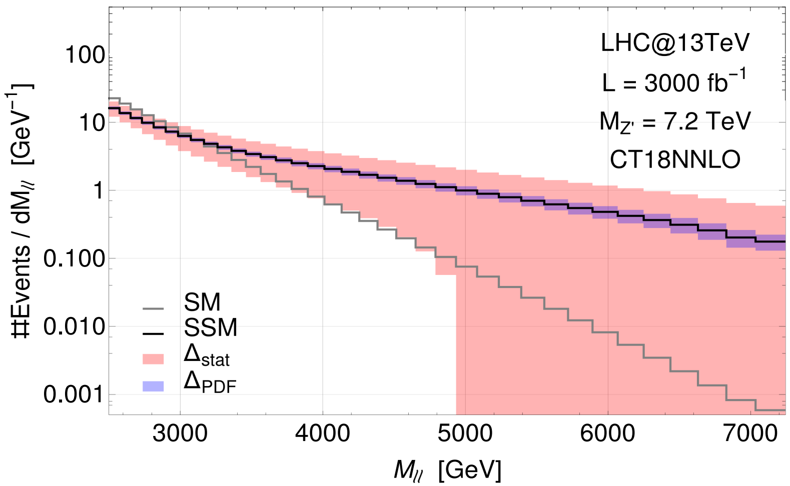

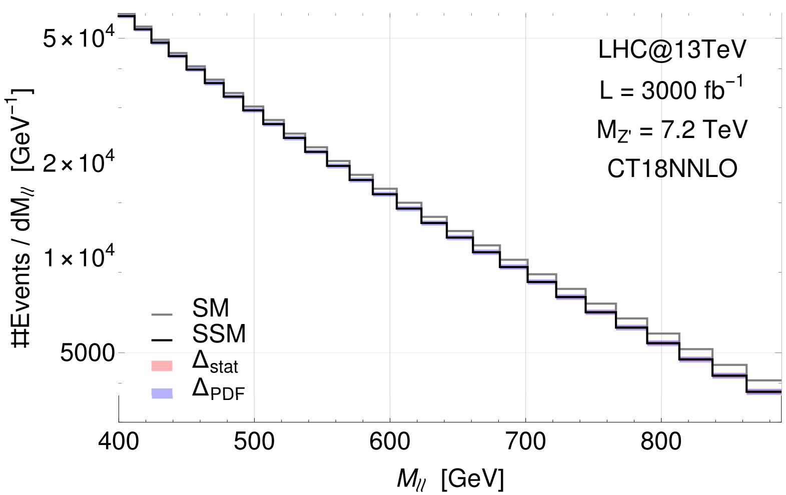

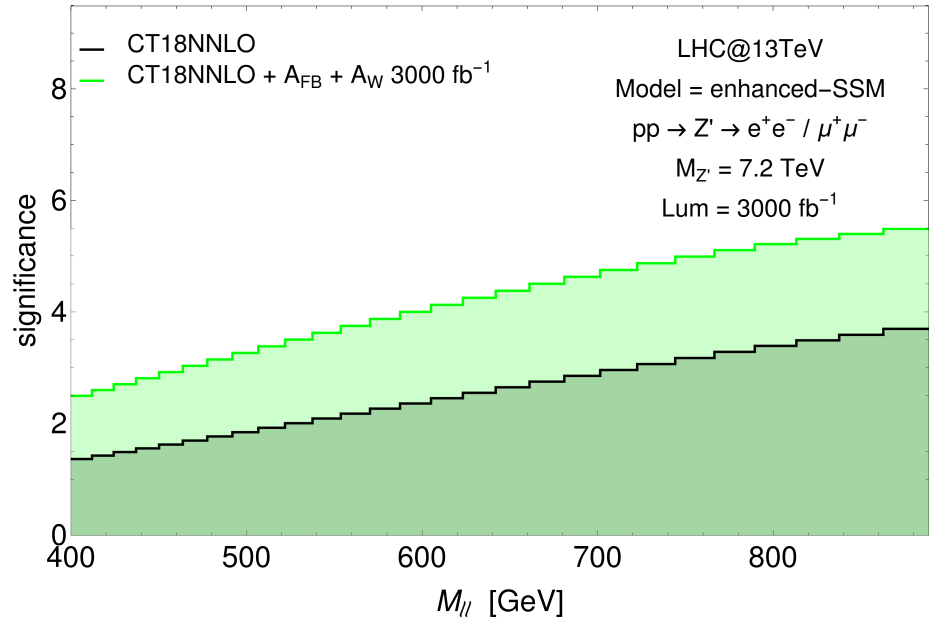

- High invariant mass excess non-significant
- Significant depletion of events in the low invariant mass region
- **Early evidence of BSM physics significantly improved by reduction of PDF uncertainty**